Supporting Information

Two Eu-Doped Polyoxotungstates with Distinct Structures for Multifunctional Integration of Photoluminescence, Proton Conductivity and Resistive Switching

Wen-Jun Mi, [a] Xue-Ru Zhou, [a] Guang-Qu Ke, [a] Bi-Ling Huang, [a] Yi-Ping Chen,* [a, b] Hao-Hong Li [a]

[a] College of Chemistry, Fuzhou University, Fuzhou, Fujian 350108, China.

[b] State Key Laboratory of Structural Chemistry, Fujian Institute of Research on the Structure of Matter, Chinese Academy of Sciences, Fuzhou 350002, China.

Contents

Section S1 Experimental Detail

Materials and physical measurements. $K_8Na_2[A\text{-}a\text{-}GeW_9O_{34}]\cdot 25H_2O$ was synthesized according to the reported procedure. Other chemicals are purchased commercially and used without purification. The infrared spectra in the range of 400-4000 cm^{-1} were measured on the Thermo Scientific Nicolet iS50 FT-IR spectrometer by KBr pellets at room temperature. 2D COS-IR was measured on the same instrument equipped with a portable programmable temperature controller (Love Control Corporation) with an operating temperature range of 20 °C to 120 °C, and the magnetic controller with a varying magnetic intensity of 5-50 mT was designed by our group. The X-ray powder diffraction data were measured on a Rigaku UItima IV X-Ray Diffractometer powder diffractometer, with the Cu-Kα radiation angular range of 5-55° and the radiation wavelength of 1.54056 Å. Solid-state UV-vis spectra were measured on a Perkin-Elmer Lambda 800 instrument with a scanning range of 200-800 nm. Thermogravimetric analysis (TGA) was performed using a Mettler Toledo Star TGA /DSCI analyzer under a nitrogen atmosphere at the heating rate of 10 K min^{-1}. The instrument used for the determination of XPS (X-ray photoelectron spectroscopy) was an ESCALAB 250 photoelectron spectrometer from VG Corporation USA, with Al-Kα as the target ray source. Luminescent spectra were collected with an Edinburgh Instruments FS980 TCSPC luminescence spectrometer on the powdered crystal material of the compounds. The measurement of proton conductivity is carried out using alternating current impedance spectroscopy with a dual electrode configuration between 10^7 and 0.1Hz. The temperature range is 25 ~ 85 ℃, and the relative humidity (RH) range is 55 ~ 98% RH. Use the formula $\sigma = L/(RS)$ to calculate the conductivity (L, R, S represent thickness (cm), fitting resistance (Ω), and cross-sectional area (cm^2), respectively. Ac impedance measurements were carried out with a SI1260 IMPEDANCE/GAINPHASE analyzer over the frequency range from 1 Hz to 10 MHz with an applied voltage of 10 mV. The relative humidity was controlled by a STIKCorp CIHI-150BS3 incubator. The samples were pressed to form a cylindrical pellet of the crystalline powder sample (~1.0 mm thickness × 5/4.5 mm ϕ) coated with C-pressed electrodes. Two silver electrodes were attached to both sides of the pellet to form four end terminals (quasi-four-probe method). The bulk conductivity was estimated by semicircle fittings of Nyquist plots. The resistive switching performances were measured by recording the current-voltage (*I-V*) curves on a Keysight B2911A single channel digital source meter.

Synthesis of 1-Eu: $K_8Na_2[A\text{-}\alpha\text{-}GeW_9O_{34}]\cdot 25H_2O$ (0.50g, 0.20mmol), $Eu(NO_3)_3\cdot 6H_2O$ (0.120g, 0.355mmol) and KCl (0.050 g, 0.670 mmol) were dissolved in 3.0 mL distilled water under stirring, then 50μL of ethylenediamine and 50 μL 1M dimethylamine hydrochloride were added. The pH value of the solution was then adjusted to 8.50 by using 6M hydrochloric acid. The obtained solution was stirred for 1 hour and then heated at 140℃ for 3 days. After cooling to room temperature and washing with mother solution, colorless bulk crystals were obtained. Yield:26.8% (based on $Na_2WO_4\cdot 2H_2O$). IR for **1-Eu** (KBr, cm^{-1}): $\tilde{\nu}$ = 3386s, 3129m, 1616s, 1509s, 1321m, 1048m, 928s, 870w, 744m, 651m, 510w.

Synthesis of 2-Eu: $K_8Na_2[A\text{-}\alpha\text{-}GeW_9O_{34}]\cdot 25H_2O$ (0.60g, 0.24mmol), $Eu(NO_3)_3\cdot 6H_2O$ (0.170g, 0.503mmol), SeO_2 (0.10g, 0.901 mmol), K_2CO_3 (0.05g, 0.362mmol), $K_2B_4O_7\cdot 5H_2O$ (0.05g, 0.124mmol) and $NH_4B_5O_8\cdot 4H_2O$ (0.05g, 0.249mmol) were dissolved in 3.0 mL distilled water under stirring. Then, 50 μL of ethylenediamine was added. The pH value of the solution was then adjusted to 8.50 by using 6M hydrochloric acid, and 50 μL 1M dimethylamine hydrochloride was added. The obtained solution was stirred for 1 hour and then heated at 100℃ for 1 day. After cooling to room temperature and washing with mother solution, colorless bulk crystals were obtained. Yield:31.2% (based on $Na_2WO_4\cdot 2H_2O$). IR for **2-Eu** (KBr, cm^{-1}): $\tilde{\nu}$ = 3437s, 3147m, 1624s, 1493s, 1321m, 1089s, 940s, 867s, 794s, 747w, 695w, 453m.

Preparation of FTO/Eu-POTs/Ag Devices: The two compounds were thoroughly ground and separately ultrasonicated in deionized water for 2 hours to form homogeneous suspensions with a concentration of 2 mg/mL. Subsequently, 0.2 mL of each suspension was uniformly deposited onto FTO substrates (20 mm × 20 mm) via spin-coating at 1000 rpm, followed by annealing at 60°C for 3 hours to remove residual moisture. Finally, the top silver electrodes for all devices were fabricated by applying a 0.5 $mg\cdot mL^{-1}$ silver nanowire suspension through a shadow mask with circular apertures of approximately 0.1 cm in diameter for 1 minute. The fabricated devices were then dried in an oven at 60°C for 30 minutes to enhance adhesion. Devices denoted as FTO/**1-Eu**/Ag and FTO/**2-Eu**/Ag were prepared accordingly. Scanning electron microscopy (SEM) images revealed smooth film surfaces (Figure S12), respectively. X-ray diffraction (XRD) analysis of the devices (Figure S1c, 1f) confirmed the successful formation of the POTs active layer while indicating that the structural integrity of the POTs nano-active materials remained unaltered.

Section S2 X-Ray Crystallography

X-ray crystallography: Single-crystal X-ray diffraction. Crystals were collected on a Bruker APEX III CCD area diffractometer equipped with a fine focus, 2.0 kW sealed tube X-ray source (MoKα radiation, λ = 0.71073 Ǻ) operating at 296.15K. The empirical absorption correction was based on equivalent reflections. The single crystal data were calculated and solved by SHELXS-97 and Olex2-1.5 programs. For **1-Eu** and **2-Eu**, all atoms are corrected for anisotropy using the least square method, and only the hydrogen atoms participate in the calculation of the structure factors. Detailed crystallographic data tables for **1-Eu** and **2-Eu** are shown in Table S1. CCDC 2512610 and 2512611 contain the crystallographic data for **1-Eu** and **2-Eu**.

Table S1. Crystallographic data and structure refinements of **1-Eu** and **2-Eu**.

	1-Eu	**2-Eu**
Empirical formula	$C_4H_{80}Eu_8Ge_4K_3N_2Na_3O_{185}W_{43}$	$C_2H_{82}Eu_{22}Ge_8K_7NNa_2O_{404}Se_{24}W_{80}$
Formula weight	12666.52	27423.7
Crystal system	monoclinic	orthorhombic
Space group	C2/c	$Pna2_1$
a, Å	83.660(8)	26.845(2)
b, Å	22.102(2)	40.935(4)
c, Å	24.206(2)	46.807(4)
α, deg	90	90
β, deg	98.037(2)	90
γ, deg	90	90
V, Å^{-3}	44320(7)	51437(8)
Z	8	4
μ, mm^{-1}	25.142	22.740
F(000)	43391	47125
D_c, g cm^{-3}	3.788	3.531
T, K	297K	297K
Limiting indices	$-99 \le h \le 99$ $-26 \le k \le 26$ $-28 \le l \le 27$	$-32 \le h \le 23$ $-48 \le k \le 48$ $-55 \le l \le 55$

Reflections collected/unique	337041/39136	426244/89809
R_{int}	0.1117	0.0987
Data/restrains/parameters	39136/226/2223	89809 / 7165 / 4859
GOF on F^2	1.083	1.047
R_1, wR_2 ($I>2\sigma(I)$)[a]	0.0989/0.2316	0.0673/0.1631
R_1, wR_2 (all data)	0.1339/0.2552	0.1123/0.1957

[a] $R_1 = \sum||F_o|-|F_c||/\sum|F_o|$, [b] $wR_2 = \{\sum[w(F_o^2-F_c^2)^2]/\sum[w(F_o^2)^2]\}^{1/2}$

Section S3 Additional Table

Table S2. CShM values of Eu(III) ions in **1-Eu**.

Central atom	Coordination polyhedron	CShM
Eu1	Enneagon (D_{9h})	30.701
	Octagonal pyramid (C_{8v})	21.821
	Hexagonal bipyramid (D_{7h})	19.903
	Johnson triangular cupola (C_{3v})	12.206
	Capped cube (C_{4v})	9.267
	Spherical-relaxed capped cube (C_{4v})	9.467
	Capped square antiprism J10 (C_{4v})	2.137
	Spherical capped square antiprism (C_{4v})	2.293
	Tricapped trigonal prism J51 (D_{3h})	**1.485**
Eu2	Octagon (D_{8h})	23.489
	Heptagonal pyramid (C_{7v})	19.726
	Hexagonal bipyramid (D_{6h})	16.892
	Cube (O_h)	15.311
	Square antiprism (D_{4d})	5.286
	Triangular dodecahedron (D_{2d})	**3.945**
	Johnson gyrobifastigium J26 (D_{2d})	13.012
	Johnson elongated triangular bipyramid J14 (D_{3h})	22.602
Eu3	Enneagon (D_{9h})	31.086
	Octagonal pyramid (C_{8v})	22.225
	Hexagonal bipyramid (D_{7h})	20.107
	Johnson triangular cupola (C_{3v})	12.121
	Capped cube (C_{4v})	8.767
	Spherical-relaxed capped cube (C_{4v})	9.195
	Capped square antiprism J10 (C_{4v})	1.901
	Spherical capped square antiprism (C_{4v})	2.275
	Tricapped trigonal prism J51 (D_{3h})	**1.590**
Eu4	Octagon (D_{8h})	30.550
	Heptagonal pyramid (C_{7v})	21.297
	Hexagonal bipyramid (D_{6h})	13.636
	Cube (O_h)	10.198
	Square antiprism (D_{4d})	4.175
	Triangular dodecahedron (D_{2d})	**2.993**
	Johnson gyrobifastigium J26 (D_{2d})	12.547
	Johnson elongated triangular bipyramid J14 (D_{3h})	22.698
Eu5	Octagon (D_{8h})	29.774
	Heptagonal pyramid (C_{7v})	23.646
	Hexagonal bipyramid (D_{6h})	15.565

	Cube (O_h)	14.104
	Square antiprism (D_{4d})	4.375
	Triangular dodecahedron (D_{2d})	**2.341**
	Johnson gyrobifastigium J26 (D_{2d})	10.114
	Johnson elongated triangular bipyramid J14 (D_{3h})	24.442
Eu6	Octagon (D_{8h})	23.041
	Heptagonal pyramid (C_{7v})	19.327
	Hexagonal bipyramid (D_{6h})	16.392
	Cube (O_h)	16.853
	Square antiprism (D_{4d})	6.199
	Triangular dodecahedron (D_{2d})	**5.097**
	Johnson gyrobifastigium J26 (D_{2d})	12.285
	Johnson elongated triangular bipyramid J14 (D_{3h})	21.820
Eu7	Octagon (D_{8h})	31.318
	Heptagonal pyramid (C_{7v})	21.970
	Hexagonal bipyramid (D_{6h})	14.140
	Cube (O_h)	10.237
	Square antiprism (D_{4d})	3.330
	Triangular dodecahedron (D_{2d})	**2.426**
	Johnson gyrobifastigium J26 (D_{2d})	12.980
	Johnson elongated triangular bipyramid J14 (D_{3h})	24.690
Eu8	Octagon (D_{8h})	31.122
	Heptagonal pyramid (C_{7v})	23.143
	Hexagonal bipyramid (D_{6h})	16.516
	Cube (O_h)	13.868
	Square antiprism (D_{4d})	4.903
	Triangular dodecahedron (D_{2d})	**2.482**
	Johnson gyrobifastigium J26 (D_{2d})	10.898
	Johnson elongated triangular bipyramid J14 (D_{3h})	24.129

Table S3. CShM values of Eu(III) ions in **2-Eu**.

Central atom	Coordination polyhedron	CShM
Eu1	Octagon (D_{8h})	31.001
	Heptagonal pyramid (C_{7v})	23.736
	Hexagonal bipyramid (D_{6h})	14.608
	Cube (O_h)	10.289
	Square antiprism (D_{4d})	3.099
	Triangular dodecahedron (D_{2d})	**2.214**
	Johnson gyrobifastigium J26 (D_{2d})	10.722
	Johnson elongated triangular bipyramid J14 (D_{3h})	24.493

	Enneagon (D_{9h})	30.878
	Octagonal pyramid (C_{8v})	22.158
	Hexagonal bipyramid (D_{7h})	17.412
	Johnson triangular cupola (C_{3v})	10.363
Eu2	Capped cube (C_{4v})	8.125
	Spherical-relaxed capped cube (C_{4v})	7.384
	Capped square antiprism J10 (C_{4v})	2.650
	Spherical capped square antiprism (C_{4v})	2.137
	Tricapped trigonal prism J51 (D_{3h})	**1.819**
	Enneagon (D_{9h})	34.502
	Octagonal pyramid (C_{8v})	22.383
	Hexagonal bipyramid (D_{7h})	17.130
	Johnson triangular cupola (C_{3v})	13.642
Eu3	Capped cube (C_{4v})	8.961
	Spherical-relaxed capped cube (C_{4v})	7.712
	Capped square antiprism J10 (C_{4v})	2.684
	Spherical capped square antiprism (C_{4v})	**1.797**
	Tricapped trigonal prism J51 (D_{3h})	3.027
	Octagon (D_{8h})	31.120
	Heptagonal pyramid (C_{7v})	23.167
	Hexagonal bipyramid (D_{6h})	16.335
Eu4	Cube (O_h)	11.735
	Square antiprism (D_{4d})	3.276
	Triangular dodecahedron (D_{2d})	**0.910**
	Johnson gyrobifastigium J26 (D_{2d})	11.543
	Johnson elongated triangular bipyramid J14 (D_{3h})	27.018
	Enneagon (D_{9h})	31.938
	Octagonal pyramid (C_{8v})	21.950
	Hexagonal bipyramid (D_{7h})	19.627
	Johnson triangular cupola (C_{3v})	12.622
Eu5	Capped cube (C_{4v})	10.102
	Spherical-relaxed capped cube (C_{4v})	9.369
	Capped square antiprism J10 (C_{4v})	1.779
	Spherical capped square antiprism (C_{4v})	**1.263**
	Tricapped trigonal prism J51 (D_{3h})	1.987
	Octagon (D_{8h})	31.767
	Heptagonal pyramid (C_{7v})	23.789
Eu6	Hexagonal bipyramid (D_{6h})	14.712
	Cube (O_h)	13.088
	Square antiprism (D_{4d})	3.478

	Triangular dodecahedron (D_{2d})	**1.256**
	Johnson gyrobifastigium J26 (D_{2d})	9.727
	Johnson elongated triangular bipyramid J14 (D_{3h})	27.334
Eu7	Octagon (D_{8h})	31.632
	Heptagonal pyramid (C_{7v})	22.793
	Hexagonal bipyramid (D_{6h})	15.904
	Cube (O_h)	11.486
	Square antiprism (D_{4d})	3.318
	Triangular dodecahedron (D_{2d})	**0.925**
	Johnson gyrobifastigium J26 (D_{2d})	11.367
	Johnson elongated triangular bipyramid J14 (D_{3h})	27.582
Eu8	Octagon (D_{8h})	30.310
	Heptagonal pyramid (C_{7v})	23.981
	Hexagonal bipyramid (D_{6h})	15.355
	Cube (O_h)	12.161
	Square antiprism (D_{4d})	2.749
	Triangular dodecahedron (D_{2d})	**1.886**
	Johnson gyrobifastigium J26 (D_{2d})	10.169
	Johnson elongated triangular bipyramid J14 (D_{3h})	26.385
Eu9	Octagon (D_{8h})	30.505
	Heptagonal pyramid (C_{7v})	24.365
	Hexagonal bipyramid (D_{6h})	15.233
	Cube (O_h)	11.992
	Square antiprism (D_{4d})	2.837
	Triangular dodecahedron (D_{2d})	**2.015**
	Johnson gyrobifastigium J26 (D_{2d})	10.005
	Johnson elongated triangular bipyramid J14 (D_{3h})	26.065
Eu10	Octagon (D_{8h})	28.723
	Heptagonal pyramid (C_{7v})	20.866
	Hexagonal bipyramid (D_{6h})	17.248
	Cube (O_h)	13.445
	Square antiprism (D_{4d})	3.943
	Triangular dodecahedron (D_{2d})	**3.105**
	Johnson gyrobifastigium J26 (D_{2d})	13.091
	Johnson elongated triangular bipyramid J14 (D_{3h})	24.507
Eu11	Octagon (D_{8h})	30.325
	Heptagonal pyramid (C_{7v})	23.793
	Hexagonal bipyramid (D_{6h})	14.931
	Cube (O_h)	13.220
	Square antiprism (D_{4d})	3.741

	Triangular dodecahedron (D_{2d})	**1.391**
	Johnson gyrobifastigium J26 (D_{2d})	10.367
	Johnson elongated triangular bipyramid J14 (D_{3h})	26.537
Eu12	Octagon (D_{8h})	31.766
	Heptagonal pyramid (C_{7v})	24.470
	Hexagonal bipyramid (D_{6h})	15.576
	Cube (O_h)	12.995
	Square antiprism (D_{4d})	3.275
	Triangular dodecahedron (D_{2d})	**1.619**
	Johnson gyrobifastigium J26 (D_{2d})	9.989
	Johnson elongated triangular bipyramid J14 (D_{3h})	27.573
Eu13	Octagon (D_{8h})	32.036
	Heptagonal pyramid (C_{7v})	23.520
	Hexagonal bipyramid (D_{6h})	15.453
	Cube (O_h)	12.841
	Square antiprism (D_{4d})	3.276
	Triangular dodecahedron (D_{2d})	**1.458**
	Johnson gyrobifastigium J26 (D_{2d})	10.552
	Johnson elongated triangular bipyramid J14 (D_{3h})	26.545
Eu14	Enneagon (D_{9h})	31.621
	Octagonal pyramid (C_{8v})	23.328
	Hexagonal bipyramid (D_{7h})	18.172
	Johnson triangular cupola (C_{3v})	11.287
	Capped cube (C_{4v})	8.426
	Spherical-relaxed capped cube (C_{4v})	7.654
	Capped square antiprism J10 (C_{4v})	2.592
	Spherical capped square antiprism (C_{4v})	2.040
	Tricapped trigonal prism J51 (D_{3h})	**1.701**
Eu15	Octagon (D_{8h})	29.273
	Heptagonal pyramid (C_{7v})	20.689
	Hexagonal bipyramid (D_{6h})	17.467
	Cube (O_h)	14.141
	Square antiprism (D_{4d})	3.766
	Triangular dodecahedron (D_{2d})	**3.070**
	Johnson gyrobifastigium J26 (D_{2d})	14.027
	Johnson elongated triangular bipyramid J14 (D_{3h})	26.241
Eu16	Octagon (D_{8h})	31.300
	Heptagonal pyramid (C_{7v})	24.024
	Hexagonal bipyramid (D_{6h})	14.897
	Cube (O_h)	9.923

	Square antiprism (D_{4d})	3.153
	Triangular dodecahedron (D_{2d})	**1.913**
	Johnson gyrobifastigium J26 (D_{2d})	11.352
	Johnson elongated triangular bipyramid J14 (D_{3h})	24.555
Eu17	Octagon (D_{8h})	29.685
	Heptagonal pyramid (C_{7v})	21.043
	Hexagonal bipyramid (D_{6h})	17.324
	Cube (O_h)	13.509
	Square antiprism (D_{4d})	3.753
	Triangular dodecahedron (D_{2d})	**3.158**
	Johnson gyrobifastigium J26 (D_{2d})	12.708
	Johnson elongated triangular bipyramid J14 (D_{3h})	24.747
Eu18	Octagon (D_{8h})	30.584
	Heptagonal pyramid (C_{7v})	23.112
	Hexagonal bipyramid (D_{6h})	16.199
	Cube (O_h)	11.833
	Square antiprism (D_{4d})	2.776
	Triangular dodecahedron (D_{2d})	**1.092**
	Johnson gyrobifastigium J26 (D_{2d})	11.650
	Johnson elongated triangular bipyramid J14 (D_{3h})	26.977
Eu19	Octagon (D_{8h})	30.678
	Heptagonal pyramid (C_{7v})	22.617
	Hexagonal bipyramid (D_{6h})	15.682
	Cube (O_h)	11.713
	Square antiprism (D_{4d})	3.196
	Triangular dodecahedron (D_{2d})	**1.064**
	Johnson gyrobifastigium J26 (D_{2d})	11.264
	Johnson elongated triangular bipyramid J14 (D_{3h})	26.590
Eu20	Octagon (D_{8h})	30.492
	Heptagonal pyramid (C_{7v})	23.104
	Hexagonal bipyramid (D_{6h})	14.786
	Cube (O_h)	12.875
	Square antiprism (D_{4d})	3.643
	Triangular dodecahedron (D_{2d})	**1.314**
	Johnson gyrobifastigium J26 (D_{2d})	9.673
	Johnson elongated triangular bipyramid J14 (D_{3h})	27.150
Eu21	Octagon (D_{8h})	30.433
	Heptagonal pyramid (C_{7v})	24.383
	Hexagonal bipyramid (D_{6h})	14.810
	Cube (O_h)	11.988

	Square antiprism (D_{4d})	2.938
	Triangular dodecahedron (D_{2d})	**2.068**
	Johnson gyrobifastigium J26 (D_{2d})	9.541
	Johnson elongated triangular bipyramid J14 (D_{3h})	25.971
Eu22	Enneagon (D_{9h})	31.905
	Octagonal pyramid (C_{8v})	22.003
	Hexagonal bipyramid (D_{7h})	19.833
	Johnson triangular cupola (C_{3v})	12.652
	Capped cube (C_{4v})	10.286
	Spherical-relaxed capped cube (C_{4v})	9.286
	Capped square antiprism J10 (C_{4v})	1.813
	Spherical capped square antiprism (C_{4v})	**1.294**
	Tricapped trigonal prism J51 (D_{3h})	2.130

Table S4. Coordination Environment of Eu(III) ions in **1-Eu**.

Eu(III) cations	Coordination environments of Eu(III) cations	Eu(III) cations	Coordination environments of Eu(III) cations
Eu1	eight O atoms from POT Bus; one μ_3-O atom shared with Eu2 and Eu7	Eu2	four O atoms from POT Bus; one μ_3-O atom shared with $\{WO_6\}$; one μ_2-O atom shared with $\{WO_4\}$; one μ_3-O atom shared with Eu1 and Eu7; one μ_2-O atom shared with Eu5
Eu3	eight O atoms from POT Bus; one μ_3-O atom shared with Eu4 and Eu6	Eu4	four O atoms from POT Bus; one μ_3-O atom shared with Eu3 and Eu6; two μ_3-O atoms shared with $\{WO_6\}$; one μ_2-O atom shared with $\{WO_4\}$
Eu5	six O atoms from POT Bus; one μ_2-O atom shared with Eu2; one μ_2-O atom shared with $\{WO_6\}$	Eu6	four O atoms from POT Bus; one μ_3-O atom shared with $\{WO_6\}$; one μ_2-O atom shared with $\{WO_4\}$; one μ_3-O atom shared with Eu3 and Eu4; one μ_2-O atom shared with Eu8
Eu7	four O atoms from POT Bus; one μ_3-O atom shared with Eu1 and Eu2; two μ_3-O atoms shared with $\{WO_6\}$; one μ_2-O atom shared with $\{WO_4\}$	Eu8	six O atoms from POT Bus; one μ_2-O atom shared with Eu2; one μ_2-O atom shared with $\{WO_6\}$

Table S5. Coordination Environment of Eu(III) ions in **2-Eu**.

Eu(III) cations	Coordination environments of Eu(III) cations	Eu(III) cations	Coordination environments of Eu(III) cations
Eu1	four O atoms from POT Bus; four μ_3-O atoms shared with $\{SeO_3^{2-}\}$	Eu2	six μ_3-O atoms shared with $\{SeO_3^{2-}\}$; three μ_2-O atoms shared with $\{SeO_3^{2-}\}$
Eu3	five μ_3-O atoms shared with $\{SeO_3^{2-}\}$; one μ_3-O atom shared with $\{SeO_3^{2-}\}$; one μ_2-O atom shared with Eu15; two O atoms from water molecules.	Eu4	four μ_3-O atoms shared with $\{SeO_3^{2-}\}$; three μ_3-O atoms shared with $\{SeO_3^{2-}\}$; one μ_2-O atom shared with $\{SeO_3^{2-}\}$
Eu5	six μ_3-O atoms shared with $\{SeO_3^{2-}\}$; three μ_2-O atoms shared with $\{SeO_3^{2-}\}$	Eu6	four O atoms from POT Bus; three μ_3-O atoms shared with $\{SeO_3^{2-}\}$; one μ_2-O atom shared with $\{SeO_3^{2-}\}$
Eu7	four μ_3-O atoms shared with $\{SeO_3^{2-}\}$; three μ_3-O atoms shared with $\{SeO_3^{2-}\}$; one μ_2-O atom shared with $\{SeO_3^{2-}\}$	Eu8	four O atoms from POT Bus; three μ_3-O atoms shared with $\{SeO_3^{2-}\}$; one μ_2-O atom shared with $\{SeO_3^{2-}\}$
Eu9	four O atoms from POT Bus; four μ_3-O atoms shared with $\{SeO_3^{2-}\}$	Eu10	four O atoms from POT Bus; four μ_3-O atoms shared with $\{SeO_3^{2-}\}$
Eu11	four O atoms from POT Bus; four μ_3-O atoms shared with $\{SeO_3^{2-}\}$	Eu12	four O atoms from POT Bus; four μ_3-O atoms shared with $\{SeO_3^{2-}\}$
Eu13	four O atoms from POT Bus; four μ_3-O atoms shared with $\{SeO_3^{2-}\}$	Eu14	six μ_3-O atoms shared with $\{SeO_3^{2-}\}$; three μ_2-O atoms shared with $\{SeO_3^{2-}\}$
Eu15	six μ_3-O atoms shared with $\{SeO_3^{2-}\}$; one μ_2-O atom shared with Eu3; one O atom from water molecule.	Eu16	four O atoms from POT Bus; four μ_3-O atoms shared with $\{SeO_3^{2-}\}$
Eu17	four O atoms from POT Bus; four μ_3-O atoms shared with $\{SeO_3^{2-}\}$	Eu18	four O atoms from POT Bus; three μ_3-O atoms shared with $\{SeO_3^{2-}\}$; one μ_2-O atom shared with $\{SeO_3^{2-}\}$
Eu19	four O atoms from POT Bus; three μ_3-O atoms shared with $\{SeO_3^{2-}\}$; one μ_2-O atom	Eu20	four O atoms from POT Bus; three μ_3-O atoms shared with $\{SeO_3^{2-}\}$; one μ_2-O atom shared

	shared with $\{SeO_3^{2-}\}$		with Eu21
Eu21	four O atoms from POT Bus; three μ_3-O atoms shared with $\{SeO_3^{2-}\}$; one μ_2-O atom shared with Eu22	Eu22	six μ_3-O atoms shared with $\{SeO_3^{2-}\}$; three μ_2-O atoms shared with $\{SeO_3^{2-}\}$

Table S6. Hydrogen bond lengths (Å) and angles(°) of compound **1-Eu**.

D—H···A	d(D—H)	d(H···A)	d(D—A)	Ang(D-H···A)°	Symmetry codes of A
O_d100-H100B···O_b22	0.850	2.295	2.9003(8)	126.926	3/2-x, 3/2-y, 1-z
O_d17-H17B···O_b121	0.850	2.890	3.2816(3)	110.148	1-x, 1-y, 1-z
O_d17-H17A···O_d104	0.850	2.922	3.2486(3)	105.076	1-x, 1-y, 1-z
C4-H4C···O_c15	0.960	1.845	2.7540(12)	156.867	x, y, z
C2-H2B···O_b63	0.960	1.909	2.8536(2)	167.523	x, y, z
C2-H2C···O_b145	0.960	1.768	2.6666(2)	154.494	x, y, z
Ow8-Hw8A···O_b95	0.850	2.015	2.8645(2)	180.000	x, y, z
Ow1-Hw1B···O_b122	0.850	1.938	2.7803(2)	170.479	x, y, z
Ow3-Hw3B···O_d139	0.850	2.168	2.8080(2)	131.931	3/2-x, 1/2+y, 3/2-z
Ow7-Hw7A···O_c50	0.850	1.846	2.6964(2)	180.000	x, y, z
Ow8-Hw8A···O_c168	0.850	2.500	2.8723(2)	108.319	x, y, z
Ow4-Hw4A···O_c40	0.850	2.047	2.8972(2)	180.000	x, 2-y, 1/2+z
Ow10-Hw10B···O_d55	0.850	3.302	3.3770(6)	90.766	1-x, 2-y, 1-z
Ow10-Hw10B···O_c120	0.850	2.105	2.880(2)	180.000	1-x, 2-y, 1-z

O_d = terminal oxygen，O_b = bridging oxygen of two octahedra with common vertices，O_c = bridging oxygen of two octahedra with common edges.

Table S7. Hydrogen bond lengths (Å) and angles(°) of compound **2-Eu**.

D—H···A	d(D—H)	d(H···A)	d(D—A)	Ang(D-H···A)°	Symmetry codes of A
Ow19-Hw19A···O_b125	0.850	1.913	2.7648(2)	180.000	x, y, z
Ow12-Hw12A···O_c182	0.850	1.997	2.8466(5)	180.000	x, y, z
Ow3-Hw3B···O_b7	0.850	2.011	2.8528(6)	180.000	x, y, z
Ow7-Hw7A···O_c367	0.850	2.039	2.8939(6)	180.000	x, y, z
Ow19-Hw19B···O_d263	0.850	2.304	2.9104(5)	128.741	-1+x, y, z
Ow19-Hw19B···O_b270	0.850	2.520	2.9206(2)	109.775	x, y, z
Ow25-Hw25B···O_c17	0.850	2.070	2.9191(5)	178.284	x, y, z
Ow3-Hw3B···O_b259	0.850	2.633	3.0087(5)	107.888	x, y, z

Ow19-Hw19B···O_b292	0.850	2.595	3.0071(8)	113.549	x, y, z
Ow17-Hw17B···O_c57	0.850	2.553	3.0106(2)	126.934	2-x, 1-y, 1/2+z
Ow10-Hw10B···O_c220	0.850	2.592	3.0218(2)	112.559	x, y, z
Ow23-Hw23B···O_c242	0.850	2.219	3.0271(7)	150.097	x, y, z
Ow26-Hw26B···O_c217	0.850	2.622	3.0329(8)	110.820	x, y, z
Ow17-Hw17B···O_d166	0.850	2.234	3.0753(1)	177.082	x, y, z
Ow17-Hw17A···O_c57	0.850	2.161	3.0106(2)	180.000	2-x, 1-y, -1/2+z
O_d310-H130B···O_c183	0.850	2.488	2.9740(7)	116.765	3/2-x, -1/2+y, 1/2+z
O_d150-H150B···O_c125	0.850	2.355	2.9502(3)	127.843	1-x, 1-y, 1/2+z
Ow13-Hw13B···O_d150	0.850	2.030	2.9820(8)	180.000	1-x, 1-y, 1/2+z
Ow13-Hw13A···O_c121	0.850	2.088	2.9351(4)	175.188	x, y, z
O343-H81A···Ow1	0.850	2.092	2.9342(8)	171.801	x, y, z
O81-H81B···O_b76	0.850	2.068	2.8028(5)	144.741	x, y, z
O331-H311A···O_b139	0.850	1.997	2.7959(5)	156.413	x, y, z

Table S8. Comparison of the PL lifetimes and quantum yield of various Eu(III)-incorporated POTs.

Compound	PL lifetime (τ*)	quantum yield (%)	Ref.
$[H_2N(CH_3)_2]_8Na_2H_4[Eu_2W_3BiO_6(HPO_3)(H_2MA)(H_2O)_5]_2[B\text{-}\alpha\text{-}SeW_9O_{33}]_4\cdot 52H_2O$	391.45 μs	-	1
$Na_4[Eu_4(H_2O)_2(H_2PDBA)_2(HPO_3)_2W_6O_{10}][B\text{-}\alpha\text{-}TeW_8O_{31}]_4\cdot 70H_2O$	749.51 μs	8.47	2
$K_6H_{36}[\{As_2W_{19}O_{68}\}_2\{W_5O_{19}(OH)Eu_5(Glu)_2(H_2O)_{15}\}\{(\alpha\text{-}AsW_9O_{33})_2W_4O_{10}(Glu)_2Eu_4(H_2O)_{17}\}_2]\cdot 90H_2O$	232.00 μs	-	3
$[H_2N(CH_3)_2]_{14}Na_{30}H_6[W_4O_{10}][B\text{-}\beta\text{-}BiW_9O_{33}]_2\{[Bi_{5.35}Sb_{0.65}Eu_3O_9(H_2O)_9][B\text{-}\alpha\text{-}SbW_9O_{33}]_3\}_2\cdot 124H_2O$	340.00 μs	-	4
$H_{36}Na_6(H_2O)_6\{[Eu_{20}(OH)_6(H_2O)_{24}(SO_3)_3(SeO_3)_9][\beta(4,11)\text{-}GeW_{10}O_{38}]_3[\beta(5,10)\text{-}GeW_{10}O_{38}]_3\}\cdot 61H_2O$	411.00 μs	22.40	5
$H_{32}[H_2N(CH_3)_2]_4[Na_7(H_2O)_7][K_{10}(H_2O)_{12}]\{Eu_4(HCOO)_4[(W_2O_2)(HCOO)(B\text{-}\alpha\text{-}SeW_7O_{28})_2][(SeO)_4(W_2O_7)_4(B\text{-}\alpha\text{-}SeW_9O_{33})_4]\}\cdot 26H_2O$	759.8 μs	-	6
$H_{21}[H_2N(CH_3)_2]_4[Na_4(H_2O)_7][K_4(H_2O)_5](EuSe_2O_2)\{(EuO_2)[(Eu(H_2O)_3](WO_2)_2(W_2O_5)(HCOO)_2\}_2\{[B\text{-}\alpha\text{-}SeW_8O_{31}]_2[B\text{-}\alpha\text{-}SeW_9O_{33}]_4\}\cdot 24H_2O$	722.8 μs	-	6

$H_{38}Na_{10}K_{14}(TMEDA)_8[Eu_{30}Ge_{12}W_{107}O_{420}(OH)_2(H_2O)_{14}]$ ·solvents	625 μs	39.09	7
1-Eu	**481.4 μs**	**15.39**	**This work**
2-Eu	**818.5 μs**	**47.34**	**This work**

Table S9 Summary of proton conductivity of POTs.

Compounds	Conductivity$_{max}$ (S·cm^{-1})	E_a (eV)	Ref
$Cs_5[Tb(H_2O)_4P_4W_6(O_2)_6(OH)_4O_{24}]\cdot nH_2O$	2.78×10^{-3} (65 °C, 95%RH)	0.49	8
$[Zn(NH_2trz)_3][NH_3trz]_2[SiW_{12}O_{40}]\cdot10H_2O$	5.6×10^{-3} (80 °C, 98%RH)	0.28	9
$Na_2(H_3O)_6[\{Ru^{IV}(bpy)\}_2\{WO_2(C_2O_4)\}_2(GeW_{11}O_{39})_2]\cdot27H_2O$	1.24×10^{-2}(80 °C, 90%RH)	0.24	10
$H_{17}(H_2en)_3[Sb^{III}_9Sb^{V}Ce_3O_{14}(H_2O)_3][(SbW_9O_{33})_3(PW_9O_{34})]\cdot28H_2O$	4.57×10^{-4}(85 °C, 98%RH)	0.34	11
$H_9[Ln_9W_8(\mu_4\text{-}O)_{12}(\mu_2\text{-}O)_{24}(H_2O)_{24}](SiW_{12}O_{40})_3\cdot60H_2O$	4.75×10^{-4}(85 °C, 98%RH)	0.76	12
$H_{38}Na_{10}K_{14}(TMEDA)_8[Eu_{30}Ge_{12}W_{107}O_{420}(OH)_2(H_2O)_{14}]\cdot$solvents	1.95×10^{-2}(85 °C, 98%RH)	0.32	7
1-Eu	**6.10×10^{-3}(85 °C, 98%RH)**	**0.29**	**This work**
2-Eu	**6.58×10^{-3}(85 °C, 98%RH)**	**0.27**	**This work**

Table S10 Summary of storage performance of POMs.

Devices structure	ON/OFF	Set /Reset (V)	Endurance	Ref.
$\{[Co_2(bpdo)_4(H_2O)_6](\alpha\text{-}GeW_{12}O_{40})\}\cdot4(H_2O)_n$	1.18×10^2	1.77/-2.10	100	13
$[Co(H_2O)_6]_2[Co_3(bpdo)_4(H_2O)_{10}][Co_4(H_2O)_2($ B-a-$PW_9O_{34})_2]\cdot2bpdo\cdot14H_2O$	27.3	-0.63/0.75	20	14
$(MV)_2[Cu_2I_3](MnMo_6O_{18}L_2)\cdot4CH_3CN$	2.328×10^2	0.97/-3.49	700	15
$H_4[Na(H_2O)_5]_2[Co^{II}(en)_3]_2\{[Co^{III}(en)]_2(Ta_6O_{19})_2\}\cdot22H_2O$	1.43×10^3	3.79/-7.64	100	16
$Na_{10}(H_2O)_{36}[Co_2(phen)_2(4,4'\text{-}bipy)(Nb_6O_{19})_2]\cdot19H_2O$	1.18×10^3	1.12/7.00	200	17
$H_{32}[H_2N(CH_3)_2]_4[Na_7(H_2O)_7][K_{10}(H_2O)_{12}]\{Eu_4(HCOO)_4[(W_2O_2)(HCOO)($B-α-$SeW_7O_{28})_2][(SeO)_4(W_2O_7)_4($B-α-$SeW_9O_{33})_4]\}\cdot26H_2O$	1.03×10^3	1.22/-7.14	150	6

$H_{21}[H_2N(CH_3)_2]_4[Na_4(H_2O)_7][K_4(H_2O)_5](EuSe_2O_2)\{(EuO_2)[(Eu(H_2O)_3](WO_2)_2(W_2O_5)(HCOO)_2\}_2\{[B\text{-}\alpha\text{-}SeW_8O_{31}]_2[B\text{-}\alpha\text{-}SeW_9O_{33}]_4\}\cdot 24H_2O$	3.67×10^3	0.94/-7.40	130	**6**
1-Eu	**4.98×10^3**	**1.00/-**	**105**	**This work**
2-Eu	**2.68×10^4**	**1.08/-7.28**	**125**	**This work**

Table S11. Bond valence calculations of the W, Eu and Se atoms in **1-Eu** and **2-Eu**.

1-Eu					
Atoms	BVS	Valence	Atoms	BVS	Valence
W1	6.13	+6	W27	5.99	+6
W2	6.09	+6	W28	6.07	+6
W3	5.71	+6	W29	6.11	+6
W4	5.99	+6	W30	6.21	+6
W5	6.21	+6	W31	6.25	+6
W6	6.07	+6	W32	5.98	+6
W7	6.49	+6	W33	5.81	+6
W8	5.43	+6	W34	5.92	+6
W9	5.86	+6	W35	6.08	+6
W10	6.57	+6	W36	6.36	+6
W11	6.04	+6	W37	5.94	+6
W12	6.20	+6	W38	6.08	+6
W13	6.03	+6	W39	5.99	+6
W14	6.30	+6	W40	6.12	+6
W15	6.34	+6	W41	5.86	+6
W16	5.97	+6	W42	6.22	+6
W17	5.86	+6	W43	6.10	+6
W18	5.83	+6	Eu1	2.99	+3
W19	5.92	+6	Eu2	2.96	+3
W20	5.82	+6	Eu3	3.03	+3
W21	5.89	+6	Eu4	3.39	+3
W22	6.03	+6	Eu5	3.20	+3
W23	6.09	+6	Eu6	2.93	+3
W24	6.16	+6	Eu7	3.09	+3
W25	5.86	+6	Eu8	3.25	+3
W26	6.25	+6			
2-Eu					
Atoms	BVS	Valence	Atoms	BVS	Valence
W1	5.71	+6	W69	6.27	+6
W2	6.21	+6	W70	5.73	+6
W3	6.61	+6	W71	5.93	+6
W4	6.85	+6	W72	6.32	+6
W5	6.26	+6	W73	6.21	+6

W6	6.41	+6	W74	6.06	+6
W7	6.14	+6	W75	5.70	+6
W8	5.80	+6	W76	5.96	+6
W9	6.41	+6	W77	6.12	+6
W10	6.16	+6	W78	5.82	+6
W11	3.90	+6	W79	6.76	+6
W12	5.84	+6	W80	5.98	+6
W13	6.13	+6	W81	6.34	+6
W14	6.69	+6	W82	6.34	+6
W15	5.81	+6	W83	5.77	+6
W16	5.75	+6	W84	5.70	+6
W17	6.17	+6	W85	5.87	+6
W18	5.59	+6	W86	6.11	+6
W19	5.71	+6	W87	5.93	+6
W20	5.94	+6	W88	6.02	+6
W21	6.37	+6	W89	6.11	+6
W22	6.81	+6	Se1	4.17	+4
W23	6.04	+6	Se2	3.66	+4
W24	5.90	+6	Se3	4.14	+4
W25	6.13	+6	Se4	3.87	+4
W26	6.20	+6	Se5	4.04	+4
W27	6.29	+6	Se6	4.17	+4
W28	5.88	+6	Se7	3.98	+4
W29	6.40	+6	Se8	4.23	+4
W30	6.82	+6	Se9	3.79	+4
W31	6.14	+6	Se10	3.94	+4
W32	5.95	+6	Se11	4.64	+4
W33	6.33	+6	Se12	3.99	+4
W34	3.97	+6	Se13	4.17	+4
W35	5.89	+6	Se14	4.05	+4
W36	6.16	+6	Se15	4.29	+4
W37	6.14	+6	Se16	3.97	+4
W38	6.37	+6	Se17	4.18	+4
W39	5.78	+6	Se18	4.00	+4
W40	5.90	+6	Se19	4.04	+4
W41	6.02	+6	Se20	4.29	+4
W42	6.21	+6	Se21	3.86	+4
W43	5.61	+6	Se22	4.20	+4
W44	5.87	+6	Se23	3.90	+4
W45	6.10	+6	Se24	4.17	+4
W46	5.57	+6	Eu1	3.33	+3
W47	5.86	+6	Eu2	2.82	+3
W48	6.31	+6	Eu3	2.83	+3
W49	6.24	+6	Eu4	3.14	+3

W50	5.97	+6	Eu5	2.76	+3
W51	5.89	+6	Eu6	2.97	+3
W52	5.83	+6	Eu7	3.37	+3
W53	5.76	+6	Eu8	3.17	+3
W54	5.92	+6	Eu9	3.20	+3
W55	6.01	+6	Eu10	3.55	+3
W56	5.95	+6	Eu11	3.20	+3
W57	6.02	+6	Eu12	3.24	+3
W58	5.80	+6	Eu13	3.15	+3
W59	5.81	+6	Eu14	2.71	+3
W60	6.00	+6	Eu15	2.77	+3
W61	5.76	+6	Eu16	3.24	+3
W62	6.34	+6	Eu17	3.30	+3
W63	6.01	+6	Eu18	3.00	+3
W64	6.46	+6	Eu19	3.27	+3
W65	6.15	+6	Eu20	3.25	+3
W66	7.32	+6	Eu21	3.06	+3
W67	5.96	+6	Eu22	2.89	+3
W68	5.96	+6			

Table S12. Selected bond lengths (Å) for compound **1-Eu** and **2-Eu**.

1-Eu			
W1-O24	1.90(3)	W23-O42	1.89(3)
W1-O32	1.87(3)	W23-O44	1.85(3)
W1-O66	2.27(3)	W23-O72	1.72(3)
W1-O90	2.23(3)	W23-O130	2.36(3)
W1-O113	1.72(3)	W23-O146	1.91(3)
W1-O138	1.73(3)	W23-O149	1.91(3)
W2-O53	1.99(3)	W24-O70	1.87(3)
W2-O64	1.75(3)	W24-O86	1.88(3)
W2-O81	2.26(3)	W24-O98	1.88(3)
W2-O93	1.83(3)	W24-O109	1.95(3)
W2-O101	1.77(3)	W24-O111	2.39(3)
W2-O120	2.01(3)	W24-O143	1.69(3)
W3-O49	1.78(3)	W25-O75	2.26(3)
W3-O66	1.80(3)	W25-O77	1.81(3)
W3-O88	1.74(3)	W25-O95	1.91(3)
W3-O125	1.77(3)	W25-O101	2.13(3)
W4-O23	2.29(3)	W25-O102	1.97(3)
W4-O62	1.88(3)	W25-O170	1.68(3)
W4-O79	1.74(3)	W26-O6	1.92(3)
W4-O104	1.75(3)	W26-O26	1.68(3)
W4-O121	1.95(3)	W26-O27	1.89(3)
W4-O155	2.08(3)	W26-O84	2.33(3)

W5-O30	2.21(3)	W26-O91	1.86(3)
W5-O129	1.86(3)	W26-O165	1.91(3)
W5-O136	1.82(3)	W27-O63	2.08(3)
W5-O144	1.73(3)	W27-O67	1.91(3)
W5-O160	1.96(3)	W27-O86	1.95(3)
W5-O85	1.93(4)	W27-O92	1.72(3)
W6-O9	1.92(3)	W27-O97	2.26(3)
W6-O51	1.86(3)	W27-O122	1.76(3)
W6-O94	1.89(3)	W28-O40	1.82(3)
W6-O100	1.74(3)	W28-O69	1.92(3)
W6-O103	2.26(3)	W28-O105	1.70(3)
W6-O154	1.90(3)	W28-O110	1.95(3)
W7-O13	1.86(3)	W28-O114	2.31(3)
W7-O25	2.33(3)	W28-O165	1.94(3)
W7-O45	1.67(3)	W29-O42	1.93(3)
W7-O57	1.91(3)	W29-O75	2.20(3)
W7-O135	1.99(3)	W29-O78	1.76(3)
W8-O1	2.14(3)	W29-O102	1.91(3)
W8-O8	1.78(2)	W29-O112	1.71(3)
W8-O20	1.88(3)	W29-O127	2.10(3)
W8-O31	1.78(3)	W30-O5	1.92(3)
W8-O98	2.04(3)	W30-O6	1.96(3)
W8-O111	2.29(3)	W30-O59	1.83(3)
W9-O18	1.87(3)	W30-O84	2.25(3)
W9-O25	2.36(3)	W30-O139	1.74(3)
W9-O34	1.78(3)	W30-O161	1.83(3)
W9-O48	1.87(3)	W31-O15	1.91(3)
W9-O62	1.96(3)	W31-O21	1.97(3)
W9-O135	1.86(3)	W31-O107	1.68(3)
W10-O7	1.84(3)	W31-O130	2.33(3)
W10-O30	2.28(3)	W31-O149	1.87(3)
W10-O57	1.86(3)	W31-O173	1.84(3)
W10-O60	1.75(3)	W32-O11	2.01(3)
W10-O160	1.87(3)	W32-O74	1.79(3)
W10-O171	1.81(4)	W32-O89	1.91(3)
W11-O51	1.96(3)	W32-O154	1.94(3)
W11-O63	1.83(3)	W32-O167	1.74(3)
W11-O70	1.94(3)	W32-O174	2.22(3)
W11-O96	1.92(3)	W33-O21	2.02(3)
W11-O103	2.28(3)	W33-O56	1.89(3)
W11-O124	1.70(3)	W33-O61	2.28(3)
W12-O19	1.74(3)	W33-O71	1.77(3)
W12-O40	2.10(3)	W33-O162	1.95(3)
W12-O68	1.76(3)	W33-O164	1.79(3)

W12-O83	2.05(3)	W34-O7	2.04(3)
W12-O114	2.29(3)	W34-O13	1.94(3)
W12-O119	1.74(3)	W34-O16	1.79(3)
W13-O94	2.00(3)	W34-O52	1.93(3)
W13-O96	1.98(3)	W34-O108	1.72(3)
W13-O99	1.81(3)	W34-O163	2.25(3)
W13-O103	2.31(3)	W35-O35	1.73(3)
W13-O128	1.73(3)	W35-O67	1.92(3)
W13-O156	1.83(3)	W35-O97	2.24(3)
W14-O44	1.96(3)	W35-O99	2.06(3)
W14-O53	1.87(3)	W35-O142	1.79(3)
W14-O81	2.29(3)	W35-O153	1.97(3)
W14-O127	1.80(3)	W36-O18	2.07(3)
W14-O137	1.67(3)	W36-O25	2.28(3)
W14-O169	1.99(3)	W36-O36	1.76(3)
W15-O55	1.72(3)	W36-O151	1.75(3)
W15-O81	2.30(3)	W36-O158	2.12(3)
W15-O120	1.86(3)	W36-O172	1.80(3)
W15-O162	1.91(3)	W37-O39	1.70(3)
W15-O169	1.79(3)	W37-O50	1.79(3)
W15-O173	1.95(3)	W37-O89	1.98(3)
W16-O15	2.18(3)	W37-O153	1.87(3)
W16-O28	1.86(3)	W37-O156	2.07(3)
W16-O106	1.71(3)	W37-O174	2.24(3)
W16-O130	2.29(3)	W38-O23	2.17(3)
W16-O134	1.75(3)	W38-O121	1.95(3)
W16-O146	1.98(3)	W38-O131	1.69(3)
W17-O27	2.01(3)	W38-O136	2.06(3)
W17-O29	1.81(3)	W38-O148	1.77(3)
W17-O59	2.05(3)	W38-O166	1.92(3)
W17-O65	1.82(3)	W39-O2	2.26(3)
W17-O84	2.31(3)	W39-O22	1.92(3)
W17-O123	1.74(3)	W39-O80	1.93(3)
W18-O14	1.73(3)	W39-O118	1.79(3)
W18-O90	1.84(3)	W39-O132	1.71(3)
W18-O117	1.79(3)	W39-O161	2.05(3)
W18-O145	1.71(3)	W40-O46	2.28(3)
W19-O52	1.93(3)	W40-O47	1.72(3)
W19-O129	2.05(3)	W40-O69	1.92(3)
W19-O133	1.75(3)	W40-O91	2.01(3)
W19-O140	1.77(3)	W40-O115	1.76(3)
W19-O163	2.26(3)	W40-O168	1.93(3)
W19-O166	1.91(3)	W41-O2	2.27(3)
W20-O1	1.89(2)	W41-O3	1.75(3)

W20-O9	1.90(3)	W41-O22	1.96(3)
W20-O11	1.96(3)	W41-O29	2.07(3)
W20-O109	1.90(3)	W41-O33	1.77(3)
W20-O111	2.34(3)	W41-O116	1.89(3)
W20-O159	1.73(3)	W42-O17	1.76(3)
W21-O56	1.96(3)	W42-O30	2.38(3)
W21-O61	2.21(3)	W42-O48	1.94(3)
W21-O73	1.74(3)	W42-O155	1.81(3)
W21-O93	2.06(3)	W42-O171	2.01(3)
W21-O95	1.94(3)	W42-O85	1.92(4)
W21-O157	1.76(3)	W43-O5	1.89(3)
W22-O4	1.68(3)	W43-O80	1.93(3)
W22-O46	2.25(3)	W43-O83	1.85(3)
W22-O65	2.11(3)	W43-O110	1.91(3)
W22-O116	1.97(3)	W43-O114	2.34(3)
W22-O152	1.75(3)	W43-O141	1.71(3)
W22-O168	1.95(3)	Eu5–O8	2.32(3)
Eu1–O1	2.63(3)	Eu5–O36	2.30(3)
Eu1–O2	2.94(3)	Eu5–O97	3.00(3)
Eu1–O11	2.51(3)	Eu5–O106	2.47(3)
Eu1–O20	2.37(3)	Eu5–O113	2.41(3)
Eu1–O33	2.36(3)	Eu5–O122	2.42(3)
Eu1–O58	2.35(3)	Eu5–O126	2.31(3)
Eu1–O68	2.34(3)	Eu5–O142	2.41(3)
Eu1–O74	2.62(3)	Eu6–O12	2.59(3)
Eu1–O118	2.34(3)	Eu6–O24	2.37(3)
Eu2–O14	2.41(3)	Eu6–O28	2.42(3)
Eu2–O20	2.41(3)	Eu6–O54	2.30(3)
Eu2–O32	2.37(3)	Eu6–O61	3.12(3)
Eu2–O50	2.44(3)	Eu6–O73	2.44(3)
Eu2–O58	2.60(3)	Eu6–O125	2.40(3)
Eu2–O74	2.36(3)	Eu6–O164	2.36(3)
Eu2–O126	2.29(3)	Eu7–O32	2.45(3)
Eu2–O174	3.02(3)	Eu7–O46	2.86(3)
Eu3–O12	2.39(3)	Eu7–O58	2.36(3)
Eu3–O15	2.56(3)	Eu7–O66	2.44(3)
Eu3–O21	2.46(3)	Eu7–O115	2.37(3)
Eu3–O28	2.38(3)	Eu7–O117	2.34(3)
Eu3–O79	2.39(3)	Eu7–O119	2.32(3)
Eu3–O148	2.37(3)	Eu7–O152	2.48(3)
Eu3–O151	2.36(3)	Eu8–O19	2.37(3)
Eu3–O164	2.64(3)	Eu8–O31	2.41(3)
Eu4–O12	2.31(3)	Eu8–O54	2.26(3)
Eu4–O16	2.35(3)	Eu8–O75	3.08(3)

Eu4–O24	2.42(3)	Eu8–O77	2.38(3)
Eu4–O49	2.40(3)	Eu8–O78	2.43(3)
Eu4–O90	2.36(3)	Eu8–O134	2.36(3)
Eu4–O140	2.37(3)	Eu8–O138	2.37(3)
Eu4–O163	2.88(3)		
Eu4–O172	2.29(3)		
2-Eu			
W1-O127	2.05(4)	W46-O109	1.81(5)
W1-O197	1.82(4)	W46-O129	2.01(4)
W1-O219	1.80(4)	W46-O255	1.98(4)
W1-O222	2.36(4)	W46-O256	2.42(4)
W1-O308	1.73(4)	W46-O276	1.84(4)
W1-O366	2.11(4)	W46-O364	1.91(4)
W2-O97	2.00(4)	W47-O100	1.96(5)
W2-O193	1.76(4)	W47-O104	1.82(4)
W2-O227	1.91(4)	W47-O120	1.95(4)
W2-O318	2.05(4)	W47-O154	1.97(5)
W2-O332	1.66(5)	W47-O166	1.70(4)
W2-O374	2.27(4)	W47-O176	2.36(4)
W3-O4	2.40(4)	W48-O32	2.07(4)
W3-O12	1.91(4)	W48-O36	2.26(4)
W3-O14	1.69(4)	W48-O44	1.91(4)
W3-O22	1.76(4)	W48-O50	1.73(4)
W3-O30	1.91(4)	W48-O64	1.95(4)
W3-O393	1.86(4)	W48-O86	1.68(4)
W4-O116	1.52(6)	W49-O255	1.87(4)
W4-O142	2.23(5)	W49-O259	1.95(4)
W4-O151	1.76(6)	W49-O291	1.86(4)
W4-O190	2.15(6)	W49-O310	1.68(4)
W4-O367	1.96(5)	W49-O352	2.43(4)
W4-O395	1.88(5)	W49-O370	1.88(5)
W5-O107	1.92(4)	W50-O29	1.96(4)
W5-O223	1.78(4)	W50-O133	1.84(4)
W5-O257	1.83(4)	W50-O272	1.94(4)
W5-O280	2.42(4)	W50-O352	2.26(4)
W5-O283	1.95(4)	W50-O370	2.01(4)
W5-O326	1.74(4)	W50-O392	1.67(4)
W6-O15	1.73(4)	W51-O92	1.85(4)
W6-O33	1.87(4)	W51-O106	1.88(4)
W6-O287	2.46(4)	W51-O124	2.31(4)
W6-O296	1.73(4)	W51-O144	1.83(4)
W6-O362	1.90(4)	W51-O206	1.97(5)
W6-O376	1.95(4)	W51-O216	1.92(5)
W7-O98	1.95(4)	W52-O51	1.77(4)

W7-O124	2.30(5)	W52-O226	2.31(4)
W7-O128	1.67(5)	W52-O246	2.00(4)
W7-O140	2.06(4)	W52-O321	1.91(4)
W7-O180	1.76(4)	W52-O345	1.95(4)
W7-O206	1.94(4)	W52-O380	1.76(4)
W8-O115	1.77(4)	W53-O3	2.07(7)
W8-O145	1.76(4)	W53-O96	2.31(5)
W8-O195	2.08(4)	W53-O108	2.03(5)
W8-O231	2.12(4)	W53-O188	1.90(5)
W8-O271	2.29(4)	W53-O192	1.73(5)
W8-O336	1.79(4)	W53-O218	1.75(5)
W9-O13	2.02(4)	W54-O234	1.89(5)
W9-O95	1.97(4)	W54-O289	1.85(5)
W9-O221	1.73(4)	W54-O294	1.67(4)
W9-O302	1.90(4)	W54-O318	1.86(4)
W9-O346	1.67(4)	W54-O356	1.94(5)
W9-O368	2.29(4)	W54-O374	2.44(4)
W10-O91	1.78(5)	W55-O106	1.99(4)
W10-O232	2.39(4)	W55-O122	1.64(4)
W10-O243	1.64(5)	W55-O130	2.15(5)
W10-O275	2.04(5)	W55-O154	1.96(4)
W10-O356	1.95(5)	W55-O176	2.32(5)
W10-O365	1.67(5)	W55-O184	1.85(4)
W11-O126	2.45(5)	W56-O127	1.86(4)
W11-O174	1.76(5)	W56-O241	1.89(4)
W11-O183	1.94(5)	W56-O242	1.93(4)
W11-O196	1.81(5)	W56-O274	1.75(4)
W12-O56	2.04(4)	W56-O330	1.95(4)
W12-O68	2.25(4)	W56-O340	2.30(4)
W12-O72	1.81(4)	W57-O65	1.76(5)
W12-O76	1.85(4)	W57-O103	2.30(4)
W12-O82	1.73(4)	W57-O201	2.02(4)
W12-O88	2.03(4)	W57-O249	1.93(5)
W13-O57	1.94(4)	W57-O267	1.83(4)
W13-O117	1.87(4)	W57-O269	1.93(5)
W13-O143	1.98(4)	W58-O126	2.37(5)
W13-O217	1.85(4)	W58-O136	1.69(5)
W13-O290	2.18(4)	W58-O170	1.79(5)
W13-O293	1.71(4)	W58-O194	1.90(5)
W14-O91	1.97(5)	W58-O196	2.00(5)
W14-O103	2.37(4)	W58-O210	2.17(5)
W14-O135	1.72(5)	W59-O73	1.82(4)
W14-O201	1.79(5)	W59-O189	1.91(5)
W14-O234	1.95(5)	W59-O232	2.24(4)

W14-O273	1.71(5)	W59-O269	1.92(5)
W15-O6	1.87(4)	W59-O359	1.69(5)
W15-O8	2.28(4)	W59-O365	2.04(4)
W15-O16	2.02(4)	W60-O55	1.75(4)
W15-O44	1.96(4)	W60-O57	1.96(4)
W15-O54	1.82(4)	W60-O99	1.64(4)
W15-O84	1.75(4)	W60-O137	2.00(4)
W16-O217	2.04(4)	W60-O286	1.90(4)
W16-O238	2.05(4)	W60-O290	2.29(4)
W16-O248	1.76(4)	W61-O132	2.46(4)
W16-O265	1.77(4)	W61-O148	1.83(4)
W16-O266	2.33(4)	W61-O162	1.94(5)
W16-O320	1.85(4)	W61-O168	1.64(5)
W17-O131	1.73(4)	W61-O172	1.89(5)
W17-O179	1.73(4)	W61-O220	2.00(5)
W17-O256	2.27(4)	W62-O94	1.68(5)
W17-O276	2.06(4)	W62-O96	2.32(6)
W17-O278	1.90(4)	W62-O158	1.91(5)
W17-O358	1.93(4)	W62-O188	1.71(6)
W18-O113	2.03(5)	W62-O194	1.92(6)
W18-O123	1.74(4)	W62-O212	2.12(6)
W18-O253	1.75(4)	W64-O61	1.96(4)
W18-O295	2.10(4)	W64-O205	1.70(4)
W18-O358	1.95(4)	W64-O228	1.67(4)
W18-O360	2.31(4)	W64-O256	2.30(4)
W19-O6	1.95(4)	W64-O278	1.93(4)
W19-O8	2.32(4)	W64-O364	2.03(4)
W19-O18	1.99(4)	W65-O211	1.88(4)
W19-O26	1.95(4)	W65-O226	2.40(4)
W19-O70	1.72(4)	W65-O240	1.92(4)
W19-O88	1.84(4)	W65-O246	1.92(4)
W20-O4	2.32(4)	W65-O279	1.71(4)
W20-O20	1.99(4)	W65-O312	1.83(4)
W20-O34	1.78(4)	W67-O126	1.97(5)
W20-O38	1.83(4)	W67-O183	1.49(6)
W20-O42	1.77(4)	W67-O210	1.88(6)
W20-O393	2.00(4)	W67-O361	2.07(5)
W21-O7	1.99(4)	W67-O369	2.08(5)
W21-O29	1.89(4)	W67-O395	1.87(6)
W21-O67	1.70(4)	W68-O27	1.74(4)
W21-O71	1.77(4)	W68-O39	1.76(4)
W21-O113	1.88(4)	W68-O121	1.91(4)
W21-O360	2.32(4)	W68-O250	1.93(4)
W22-O3	0.88(7)	W68-O281	2.30(4)

W22-O112	1.96(6)	W68-O306	2.05(4)
W22-O138	2.23(6)	W69-O25	1.95(4)
W22-O204	2.08(6)	W69-O203	1.67(4)
W23-O4	2.23(4)	W69-O233	1.76(4)
W23-O12	1.96(4)	W69-O250	1.92(4)
W23-O20	1.93(4)	W69-O257	2.04(4)
W23-O26	1.90(4)	W69-O280	2.26(4)
W23-O56	1.84(4)	W70-O95	1.89(4)
W23-O58	1.72(5)	W70-O117	2.00(4)
W24-O36	2.29(4)	W70-O238	1.87(4)
W24-O38	2.00(4)	W70-O263	1.68(4)
W24-O60	2.04(4)	W70-O264	2.04(4)
W24-O62	1.77(4)	W70-O368	2.34(4)
W24-O64	1.90(4)	W71-O124	2.38(4)
W24-O66	1.72(3)	W71-O140	1.73(5)
W25-O45	1.82(4)	W71-O148	2.03(5)
W25-O73	2.12(4)	W71-O178	1.96(5)
W25-O173	1.73(4)	W71-O208	1.76(5)
W25-O254	1.72(4)	W71-O216	1.90(5)
W25-O267	2.03(4)	W72-O53	1.67(4)
W25-O382	2.28(4)	W72-O226	2.33(4)
W26-O107	1.91(4)	W72-O241	1.95(4)
W26-O207	1.86(4)	W72-O312	1.95(4)
W26-O261	1.68(4)	W72-O345	1.89(4)
W26-O270	1.88(4)	W72-O366	1.80(4)
W26-O334	1.92(4)	W73-O120	1.91(5)
W26-O344	2.44(4)	W73-O130	1.62(5)
W27-O15	2.01(4)	W73-O150	1.71(5)
W27-O285	1.67(4)	W73-O162	1.93(5)
W27-O286	1.97(4)	W73-O176	2.35(4)
W27-O287	2.26(4)	W73-O178	1.85(5)
W27-O297	1.77(4)	W74-O69	1.70(4)
W27-O348	1.90(4)	W74-O97	1.91(4)
W28-O21	1.83(4)	W74-O236	1.74(4)
W28-O92	2.07(4)	W74-O289	2.08(4)
W28-O146	2.31(4)	W74-O316	1.96(4)
W28-O184	2.05(4)	W74-O374	2.34(4)
W28-O198	1.71(4)	W75-O134	1.76(5)
W28-O200	1.80(4)	W75-O142	2.08(5)
W29-O49	1.66(4)	W75-O156	2.38(5)
W29-O63	1.71(4)	W75-O160	1.78(5)
W29-O121	1.97(4)	W75-O323	1.77(5)
W29-O125	2.06(4)	W75-O369	2.16(5)
W29-O281	2.29(4)	W76-O101	1.84(4)

W29-O292	1.93(4)	W76-O141	1.72(4)
W30-O91	2.10(5)	W76-O211	1.95(4)
W30-O232	2.48(5)	W76-O251	1.92(4)
W30-O243	1.61(5)	W76-O300	2.45(4)
W30-O275	1.78(5)	W76-O354	1.88(4)
W30-O356	1.74(5)	W77-O98	1.90(4)
W30-O365	1.96(5)	W77-O102	1.76(4)
W31-O17	1.94(4)	W77-O132	2.26(5)
W31-O111	1.67(4)	W77-O152	1.71(5)
W31-O195	1.87(4)	W77-O182	1.94(4)
W31-O213	1.92(4)	W77-O220	2.06(4)
W31-O334	1.93(4)	W78-O3	2.14(7)
W31-O344	2.27(4)	W78-O112	2.02(6)
W32-O199	1.75(3)	W78-O138	1.66(5)
W32-O258	1.85(4)	W78-O151	2.24(5)
W32-O282	1.74(3)	W78-O204	1.85(5)
W32-O300	2.30(4)	W78-O367	1.67(6)
W32-O311	2.01(4)	W79-O116	2.05(6)
W32-O354	2.02(4)	W79-O142	1.76(5)
W33-O33	2.04(4)	W79-O151	2.32(5)
W33-O177	1.70(4)	W79-O190	1.60(6)
W33-O215	1.69(4)	W79-O367	2.04(5)
W33-O287	2.26(4)	W79-O395	1.80(5)
W33-O302	1.97(4)	W80-O35	1.72(4)
W33-O348	1.94(4)	W80-O61	1.90(4)
W34-O112	1.89(5)	W80-O272	1.94(4)
W34-O116	1.94(5)	W80-O284	1.79(4)
W34-O151	2.30(5)	W80-O291	2.05(4)
W34-O214	1.71(6)	W80-O352	2.25(4)
W35-O8	2.39(4)	W81-O3	1.74(7)
W35-O10	1.91(4)	W81-O112	1.87(6)
W35-O16	1.86(4)	W81-O138	1.80(5)
W35-O18	1.91(4)	W81-O151	2.34(5)
W35-O28	1.73(4)	W81-O204	1.77(5)
W35-O30	1.93(4)	W81-O367	2.08(6)
W36-O71	2.11(4)	W82-O126	2.38(5)
W36-O133	2.09(4)	W82-O183	2.00(5)
W36-O139	1.77(4)	W82-O210	1.76(5)
W36-O235	1.72(4)	W82-O361	1.62(5)
W36-O304	1.74(4)	W82-O369	1.66(5)
W36-O322	2.29(4)	W82-O395	2.04(5)
W37-O17	1.98(4)	W83-O90	1.77(4)
W37-O149	1.65(4)	W83-O100	1.86(5)
W37-O207	2.07(4)	W83-O132	2.29(4)

W37-O277	1.78(4)	W83-O172	2.04(5)
W37-O292	1.94(4)	W83-O182	2.00(5)
W37-O344	2.24(4)	W83-O202	1.78(5)
W38-O37	1.70(4)	W84-O191	1.90(4)
W38-O189	1.99(5)	W84-O225	1.75(4)
W38-O232	2.28(5)	W84-O240	1.91(4)
W38-O275	2.00(4)	W84-O251	1.91(4)
W38-O301	1.72(4)	W84-O330	1.92(4)
W38-O316	1.88(4)	W84-O340	2.42(4)
W39-O137	1.88(4)	W85-O125	1.86(4)
W39-O143	1.90(4)	W85-O270	1.99(4)
W39-O245	1.75(4)	W85-O281	2.45(4)
W39-O290	2.38(4)	W85-O283	1.92(4)
W39-O376	1.93(4)	W85-O299	1.72(4)
W39-O377	1.91(4)	W85-O306	1.86(4)
W40-O191	1.98(4)	W86-O25	1.93(4)
W40-O229	1.77(3)	W86-O213	1.92(4)
W40-O230	1.69(4)	W86-O223	2.06(4)
W40-O242	1.98(4)	W86-O231	1.77(4)
W40-O258	1.96(4)	W86-O262	1.69(4)
W40-O340	2.31(4)	W86-O280	2.29(4)
W41-O103	2.30(4)	W88-O13	1.88(4)
W41-O147	1.72(4)	W88-O59	1.73(4)
W41-O209	1.71(5)	W88-O264	1.83(5)
W41-O227	1.90(4)	W88-O362	1.95(4)
W41-O249	1.97(4)	W88-O368	2.41(4)
W41-O273	2.16(4)	W88-O377	1.94(4)
W42-O94	1.77(5)	W89-O10	1.91(4)
W42-O96	2.48(5)	W89-O22	2.07(4)
W42-O158	1.77(5)	W89-O24	1.68(4)
W42-O188	1.99(5)	W89-O32	1.80(4)
W42-O194	1.70(5)	W89-O36	2.43(4)
W42-O212	2.09(5)	W89-O60	1.87(4)
W43-O96	2.41(5)	Eu11–O83	2.47(4)
W43-O108	1.95(5)	Eu11–O90	2.38(5)
W43-O186	1.69(5)	Eu11–O104	2.21(4)
W43-O212	1.79(5)	Eu11–O118	2.42(4)
W43-O2	2.23(3)	Eu11–O146	2.70(4)
W43-O23	2.23(3)	Eu11–O164	2.44(3)
W44-O101	2.06(3)	Eu11–O169	2.54(4)
W44-O224	1.76(3)	Eu11–O200	2.33(4)
W44-O300	2.30(4)	Eu12–O63	2.39(4)
W44-O311	1.92(4)	Eu12–O79	2.51(4)
W44-O314	1.73(4)	Eu12–O268	2.34(4)

W44-O321	1.95(4)	Eu12–O271	2.61(4)
W45-O7	1.86(4)	Eu12–O277	2.26(4)
W45-O105	1.80(4)	Eu12–O305	2.56(4)
W45-O129	1.81(4)	Eu12–O307	2.40(4)
W45-O259	1.91(4)	Eu12–O336	2.34(4)
W45-O295	1.87(4)	Eu13–O39	2.33(4)
W45-O360	2.37(4)	Eu13–O85	2.46(4)
Eu1–O40	2.29(3)	Eu13–O145	2.36(4)
Eu1–O42	2.30(4)	Eu13–O233	2.30(4)
Eu1–O62	2.33(4)	Eu13–O271	2.67(4)
Eu1–O68	2.71(4)	Eu13–O307	2.37(4)
Eu1–O72	2.30(4)	Eu13–O315	2.48(4)
Eu1–O74	2.45(4)	Eu13–O329	2.50(3)
Eu1–O78	2.44(3)	Eu14–O5	2.31(4)
Eu1–O80	2.55(4)	Eu14–O87	2.43(4)
Eu2–O83	2.60(4)	Eu14–O175	2.47(4)
Eu2–O153	2.65(4)	Eu14–O298	2.68(4)
Eu2–O157	2.61(4)	Eu14–O315	2.58(4)
Eu2–O159	2.26(4)	Eu14–O329	2.58(4)
Eu2–O163	2.43(4)	Eu14–O337	2.31(4)
Eu2–O164	2.54(4)	Eu14–O349	2.62(4)
Eu2–O167	2.45(4)	Eu14–O353	2.41(3)
Eu2–O317	2.33(4)	Eu15–O41	2.30(4)
Eu2–O363	2.31(4)	Eu15–O161	2.40(3)
Eu3–O46	2.57(4)	Eu15–O268	2.52(4)
Eu3–O48	2.45(4)	Eu15–O305	2.48(4)
Eu3–O81	2.48(4)	Eu15–O331	2.52(4)
Eu3–O110	2.59(4)	Eu15–O333	2.62(4)
Eu3–O181	2.31(4)	Eu15–O342	2.41(3)
Eu3–O327	2.39(3)	Eu15–O372	2.59(4)
Eu3–O333	2.49(4)	Eu16–O19	2.51(4)
Eu3–O343	2.46(4)	Eu16–O228	2.42(4)
Eu3–O351	2.48(4)	Eu16–O284	2.30(4)
Eu4–O119	2.45(3)	Eu16–O304	2.35(4)
Eu4–O197	2.32(4)	Eu16–O319	2.46(4)
Eu4–O199	2.39(4)	Eu16–O322	2.71(4)
Eu4–O222	2.64(4)	Eu16–O325	2.41(3)
Eu4–O229	2.31(4)	Eu16–O350	2.27(3)
Eu4–O260	2.60(4)	Eu17–O31	2.39(4)
Eu4–O303	2.33(3)	Eu17–O123	2.29(4)
Eu4–O338	2.46(3)	Eu17–O139	2.35(4)
Eu5–O11	2.32(4)	Eu17–O179	2.34(4)
Eu5–O19	2.61(4)	Eu17–O322	2.63(4)
Eu5–O77	2.45(4)	Eu17–O342	2.43(4)

Eu5–O89	2.42(3)	Eu17–O350	2.39(3)
Eu5–O171	2.66(4)	Eu17–O372	2.48(4)
Eu5–O252	2.32(4)	Eu18–O147	2.36(4)
Eu5–O288	2.56(4)	Eu18–O175	2.39(4)
Eu5–O319	2.55(4)	Eu18–O193	2.37(4)
Eu5–O341	2.51(4)	Eu18–O244	2.42(4)
Eu6–O177	2.50(4)	Eu18–O247	2.63(4)
Eu6–O221	2.31(4)	Eu18–O254	2.38(4)
Eu6–O239	2.61(4)	Eu18–O298	2.41(4)
Eu6–O265	2.33(4)	Eu18–O382	2.64(4)
Eu6–O266	2.65(4)	Eu19–O37	2.32(4)
Eu6–O324	2.46(4)	Eu19–O45	2.25(4)
Eu6–O328	2.39(4)	Eu19–O75	2.60(4)
Eu6–O355	2.41(4)	Eu19–O236	2.40(4)
Eu7–O51	2.26(4)	Eu19–O244	2.36(4)
Eu7–O153	2.38(3)	Eu19–O288	2.44(4)
Eu7–O163	2.43(4)	Eu19–O341	2.37(4)
Eu7–O165	2.60(4)	Eu19–O382	2.66(4)
Eu7–O219	2.29(4)	Eu20–O43	2.55(4)
Eu7–O222	2.54(3)	Eu20–O94	2.41(5)
Eu7–O224	2.36(4)	Eu20–O134	2.46(5)
Eu7–O303	2.41(4)	Eu20–O156	2.68(5)
Eu8–O55	2.32(4)	Eu20–O157	2.50(4)
Eu8–O77	2.40(4)	Eu20–O167	2.40(4)
Eu8–O155	2.57(4)	Eu20–O170	2.26(5)
Eu8–O171	2.50(4)	Eu20–O309	2.21(4)
Eu8–O266	2.60(4)	Eu21–O87	2.38(4)
Eu8–O297	2.36(4)	Eu21–O138	2.36(5)
Eu8–O320	2.33(4)	Eu21–O156	2.61(5)
Eu8–O328	2.36(4)	Eu21–O218	2.38(5)
Eu9–O21	2.29(4)	Eu21–O309	2.32(4)
Eu9–O48	2.37(4)	Eu21–O323	2.37(5)
Eu9–O102	2.37(4)	Eu21–O339	2.53(5)
Eu9–O110	2.62(4)	Eu21–O349	2.61(4)
Eu9–O114	2.48(4)	Eu22–O74	2.56(4)
Eu9–O118	2.33(4)	Eu22–O80	2.50(4)
Eu9–O146	2.63(4)	Eu22–O119	2.46(3)
Eu9–O180	2.36(4)	Eu22–O237	2.33(4)
Eu10–O40	2.38(3)	Eu22–O313	2.45(3)
Eu10–O46	2.48(4)	Eu22–O324	2.66(3)
Eu10–O50	2.33(4)	Eu22–O338	2.63(4)
Eu10–O52	2.41(4)	Eu22–O355	2.53(4)
Eu10–O54	2.21(4)	Eu22–O357	2.31(4)
Eu10–O68	2.58(4)	Se13-O19	1.68(3)

Eu10–O76	2.27(4)	Se13-O77	1.71(4)
Eu10–O327	2.47(4)	Se13-O325	1.71(4)
Se1-O83	1.71(4)	Se14-O155	1.68(4)
Se1-O167	1.71(4)	Se14-O171	1.69(4)
Se1-O169	1.65(4)	Se14-O341	1.73(4)
Se2-O237	1.73(4)	Se15-O247	1.73(4)
Se2-O252	1.69(4)	Se15-O298	1.65(4)
Se2-O328	1.80(4)	Se15-O315	1.66(4)
Se3-O119	1.68(3)	Se16-O303	1.77(4)
Se3-O239	1.65(4)	Se16-O317	1.70(4)
Se3-O324	1.75(4)	Se16-O357	1.66(4)
Se4-O159	1.70(4)	Se17-O153	1.72(4)
Se4-O335	1.74(4)	Se17-O164	1.71(4)
Se4-O337	1.71(4)	Se17-O165	1.64(4)
Se5-O40	1.70(4)	Se18-O78	1.64(4)
Se5-O313	1.67(3)	Se18-O80	1.70(3)
Se5-O327	1.72(3)	Se18-O355	1.67(4)
Se6-O118	1.74(4)	Se19-O74	1.69(4)
Se6-O181	1.63(4)	Se19-O260	1.67(3)
Se6-O363	1.64(3)	Se19-O338	1.71(4)
Se7-O75	1.74(4)	Se20-O11	1.68(4)
Se7-O288	1.68(4)	Se20-O244	1.72(4)
Se7-O319	1.70(4)	Se20-O353	1.64(4)
Se8-O31	1.62(4)	Se21-O89	1.70(4)
Se8-O268	1.73(4)	Se21-O342	1.72(3)
Se8-O372	1.71(4)	Se21-O350	1.76(4)
Se9-O85	1.67(4)	Se22-O110	1.70(4)
Se9-O87	1.75(4)	Se22-O114	1.66(4)
Se9-O329	1.76(4)	Se22-O351	1.70(4)
Se10-O5	1.67(4)	Se23-O79	1.70(4)
Se10-O41	1.72(4)	Se23-O161	1.72(4)
Se10-O307	1.73(3)	Se23-O305	1.72(4)
Se11-O46	1.69(4)	Se24-O175	1.73(4)
Se11-O48	1.69(4)	Se24-O339	1.65(5)
Se11-O52	1.58(4)	Se24-O349	1.69(4)
Se12-O43	1.74(4)		
Se12-O157	1.72(4)		
Se12-O163	1.66(4)		

Section S4 Additional Figure

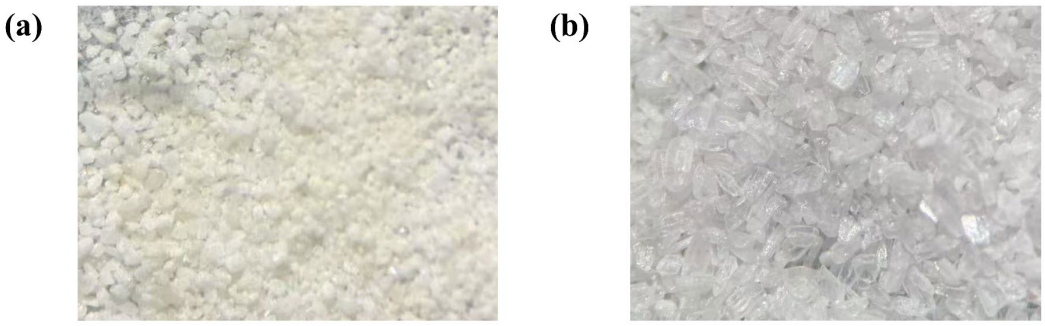

Figure S1. The photographs of the crystal morphology of **1-Eu** and **2-Eu**.

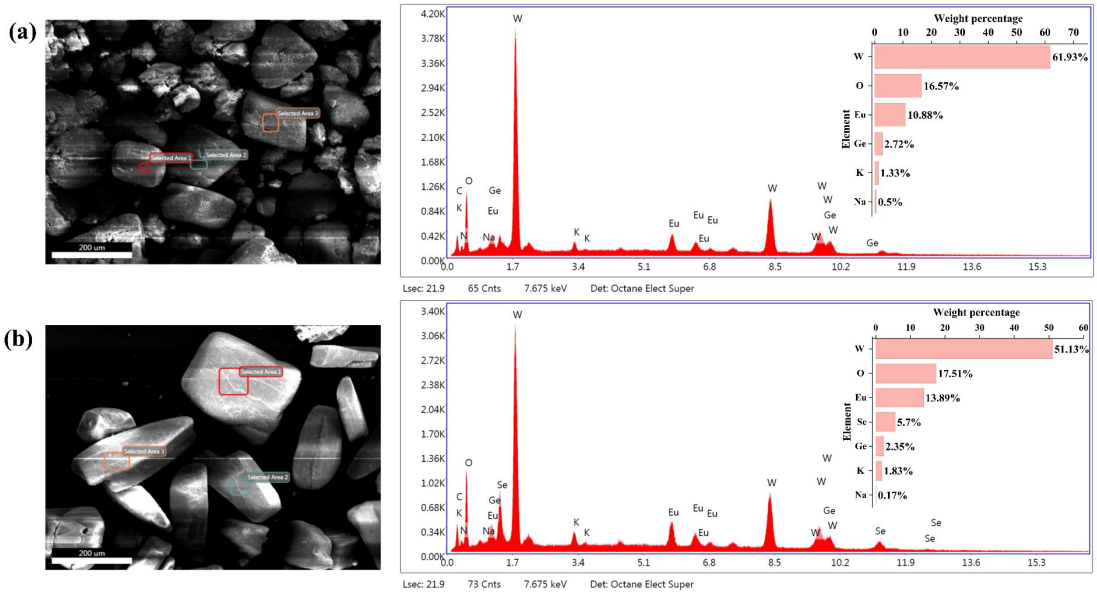

Figure S2. View of the EDS images in **1-Eu** (a) and **2-Eu** (b).

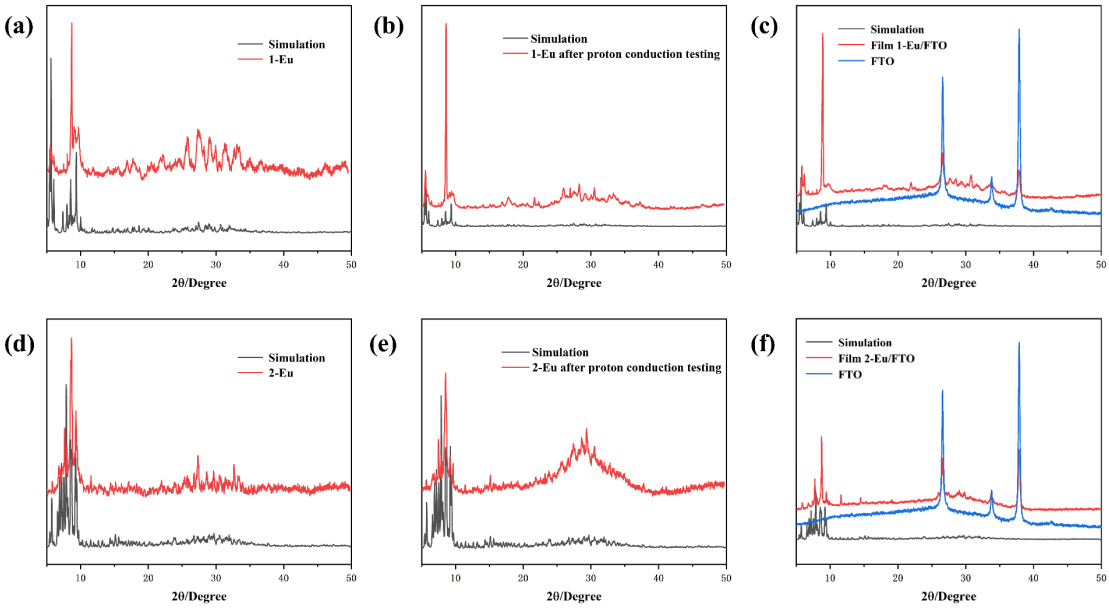

Figure S3. PXRD patterns of **1-Eu** (a) and **2-Eu** (d). Experimental PXRD pattern of **1-Eu** (b) and **2-Eu** (e) after proton conductivity test. Experimental PXRD pattern of **1-Eu** (c) and **2-Eu** (f) on FTO.

The principal peak positions in the XRD patterns of the two compounds correspond well between the theoretical simulations and the experimental measurements, while the differences in diffraction peak intensities are attributed to the anisotropic nature of the crystals.

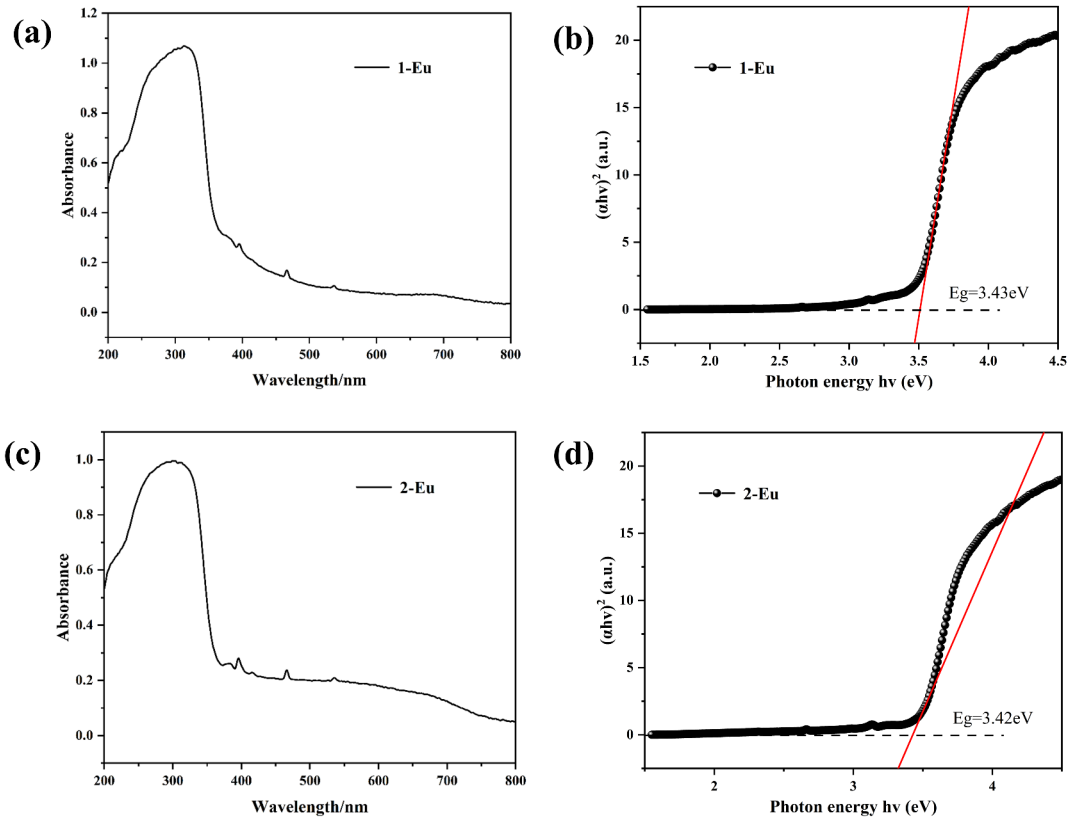

Figure S4. The UV spectrum of **1-Eu** (a) and **2-Eu** (c). Plots of $[\alpha hv]^{1/2}$ vs hv (ev) of **1-Eu** (b) and **2-Eu** (d).

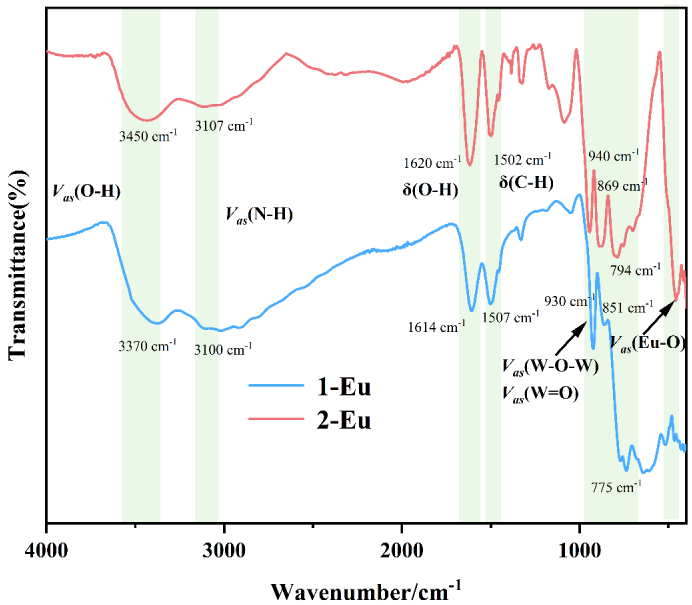

Figure S5. The IR spectrum of **1-Eu** and **2-Eu**.

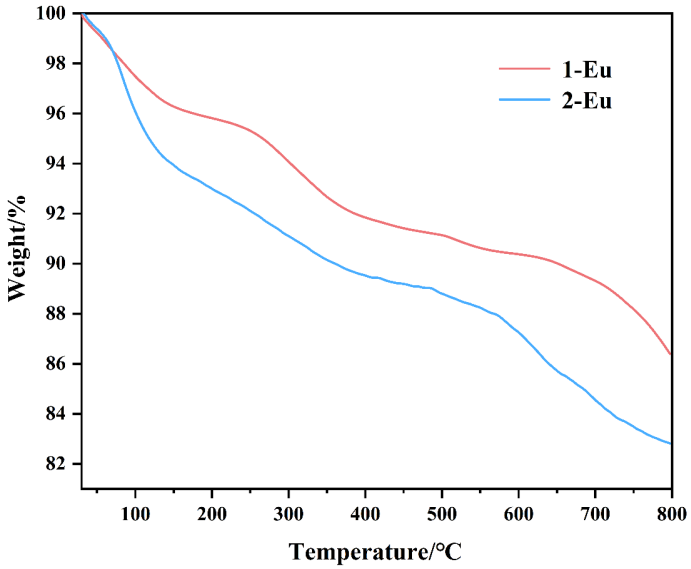

Figure S6. The thermogravimetric curve of **1-Eu** and **2-Eu**.

The thermogravimetric measurement of **1-Eu** and **2-Eu** was carried out from 30 to 800 °C under a N_2 atmosphere at a heating rate of 10 °C min^{-1}. The thermogravimetric curve suggests that **1-Eu** undergoes a two-step weight loss and **2-Eu** undergoes a one-step weight loss (Figure. S6). For **1-Eu**, the first weight loss from 30 to 400 °C 8.24 % (calcd. 8.89 %) is attributed to the liberation of 13 free water molecules, 49 solvent-water molecules and 2 protonated dimethylamine; the second weight loss from 400 to 530 °C 1.01 % (calcd. 1.06 %) is attributed to the liberation of 8 coordinated water molecules; upon heating to 530 °C, the tungsten-oxygen cluster cage skeleton is beginning to collapse. For **2-Eu**, the weight loss from 30 to 400 °C 10.29 % (calcd. 9.95 %) is attributed to the liberation of 28 free water molecules, 118 solvent-water molecules, 4 coordinated water molecules and 1 protonated dimethylamine; upon heating to 400 °C, the tungsten-oxygen cluster cage skeleton is beginning to collapse.

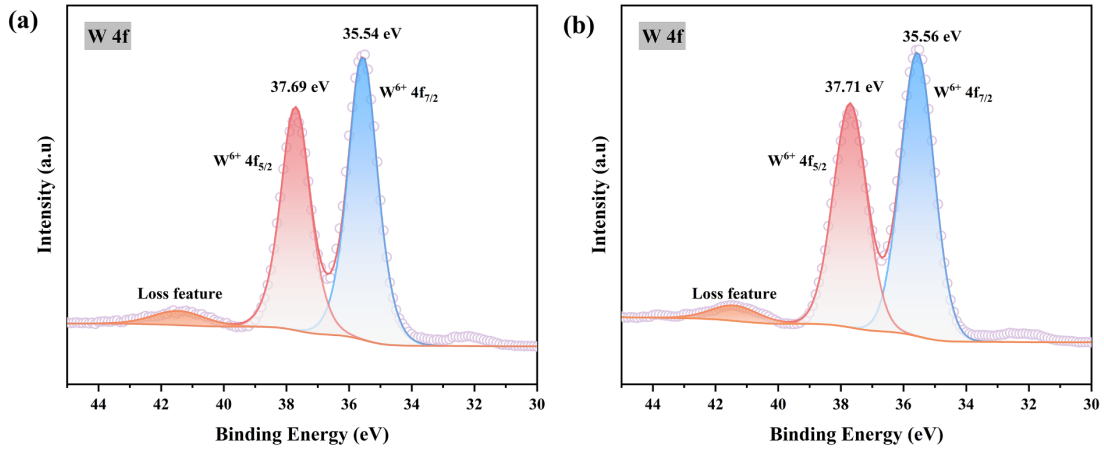

Figure S7. XPS curves of the W element of **1-Eu** (a) and **2-Eu** (b).

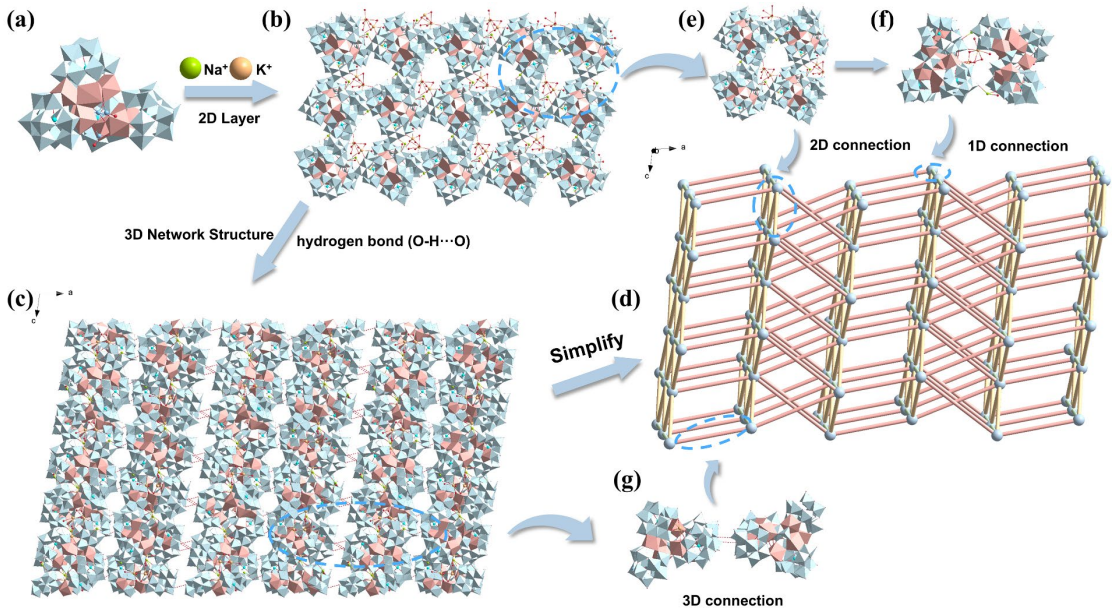

Figure S8. (a) Structure of **1-Eu**; (b) View of 2D layer; (c) View of 3D network structure; (d)The three-dimensional topology of **1-Eu**; (e) Two dimensional layered structural element; (f) One dimensional chain like structural element; (g) 3D network structure element.

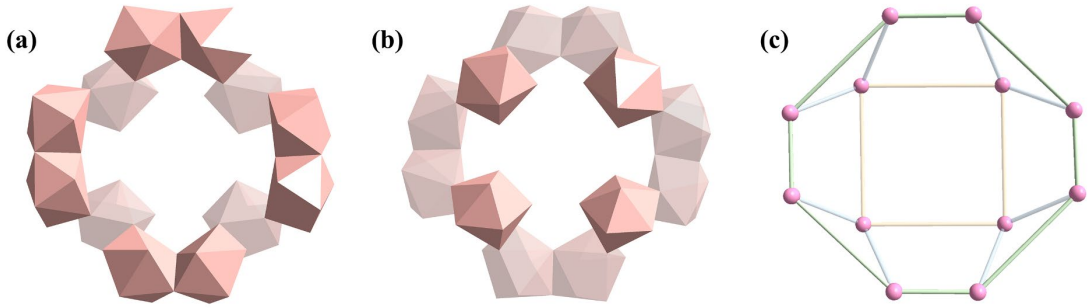

Figure S9. (a) Sub-upper structure in the $\{Eu_{12}\}$ unit; (b) Sub-substructure within the $\{Eu_{12}\}$ unit; (c) Spatial connectivity patterns of Eu ions in $\{Eu_{12}\}$.

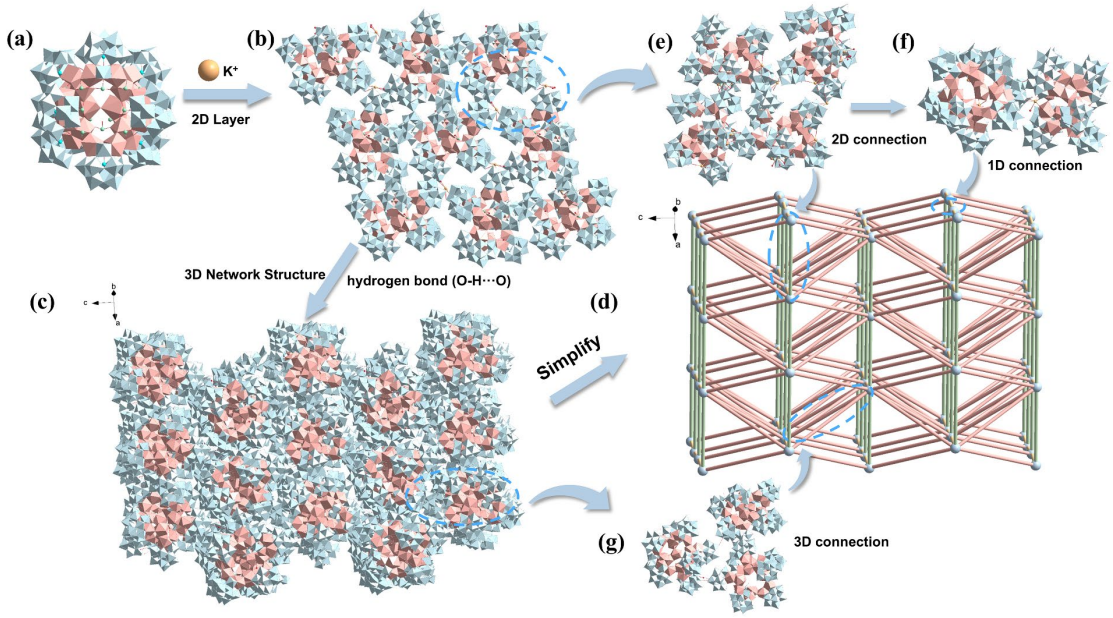

Figure S10. (a) Structure of **2-Eu**; (b) View of 2D layer; (c) View of 3D network structure; (d)The three-dimensional topology of **2-Eu**; (e) Two dimensional layered structural element; (f) One dimensional chain like structural element; (g) 3D network structure element.

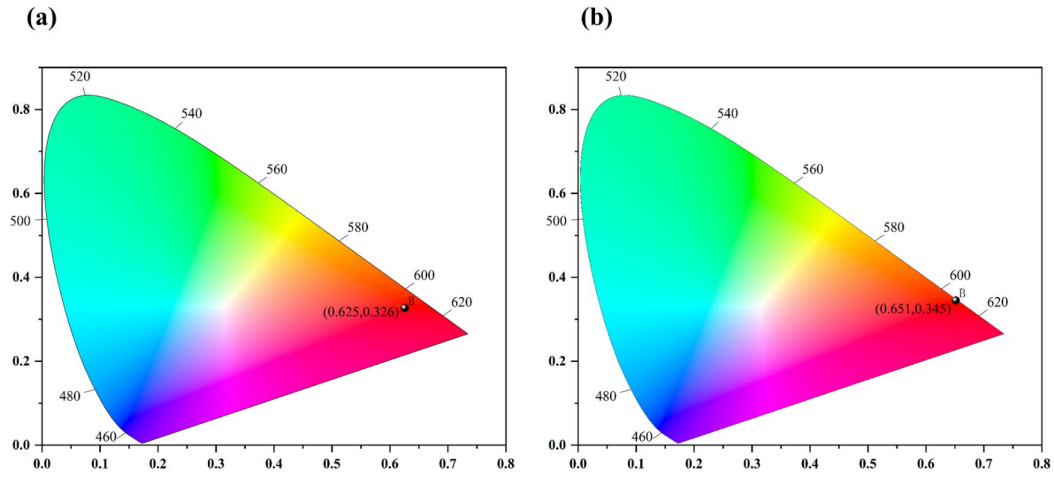

Figure. S11. The CIE of **1-Eu** (a) and **2-Eu** (b).

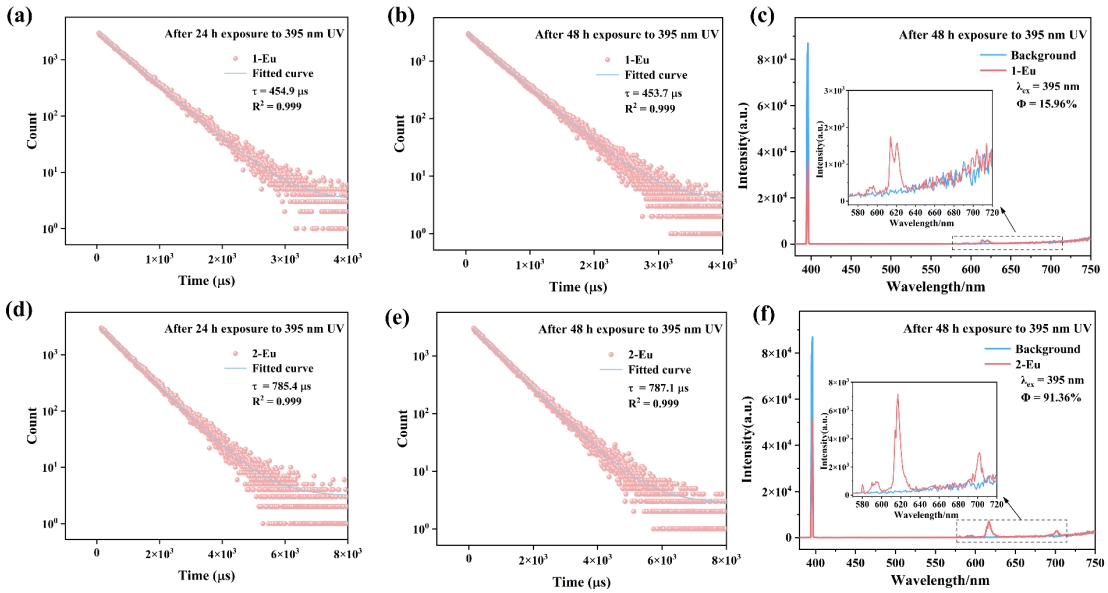

Figure S12. Lifetime decay curve of (a) **1-Eu** and (d) **2-Eu** (λ_{ex} = 395 nm) after 24 h exposure to 395 nm UV. Lifetime decay curve of (b) **1-Eu** and (e) **2-Eu** (λ_{ex} = 395 nm) after 48 h exposure to 395 nm UV. The quantum yield of (c) **1-Eu** and (f) **2-Eu** (λ_{ex} = 395 nm) after 48 h exposure to 395 nm UV.

The results show that **1-Eu** retains nearly unchanged lifetime and quantum yield after irradiation, indicating excellent photostability(Figure S12). For **2-Eu**, only a slight decrease was observed: the luminescence lifetime decreased from 818.5 μs to 785.4 μs after 24 h and 787.1 μs after 48 h, while the quantum yield decreased from 93.36% to 91.36% after 48 h(Figure S12). These results demonstrate that **2-Eu** still possesses good photostability under prolonged UV irradiation. The minor decrease in the luminescence performance of **2-Eu** may be attributed to slight photoinduced perturbations of the Eu(III) local coordination environment or the lattice microenvironment during continuous irradiation. Such subtle structural rearrangements, possibly involving weakly bound solvent molecules or hydrogen-bonding interactions, may introduce additional O-H vibrational oscillators and thus slightly increase the non-radiative decay probability.

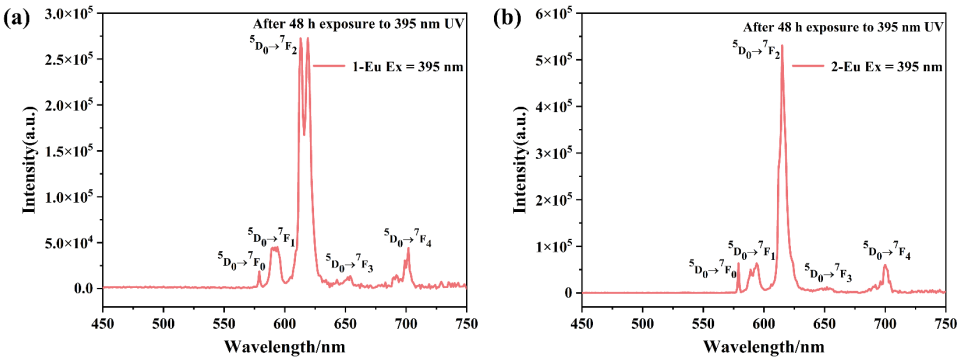

Figure S13. Emission spectra of (a) **1-Eu**; (b) **2-Eu** (λ_{ex} = 395 nm) after 48 h exposure to 395 nm UV.

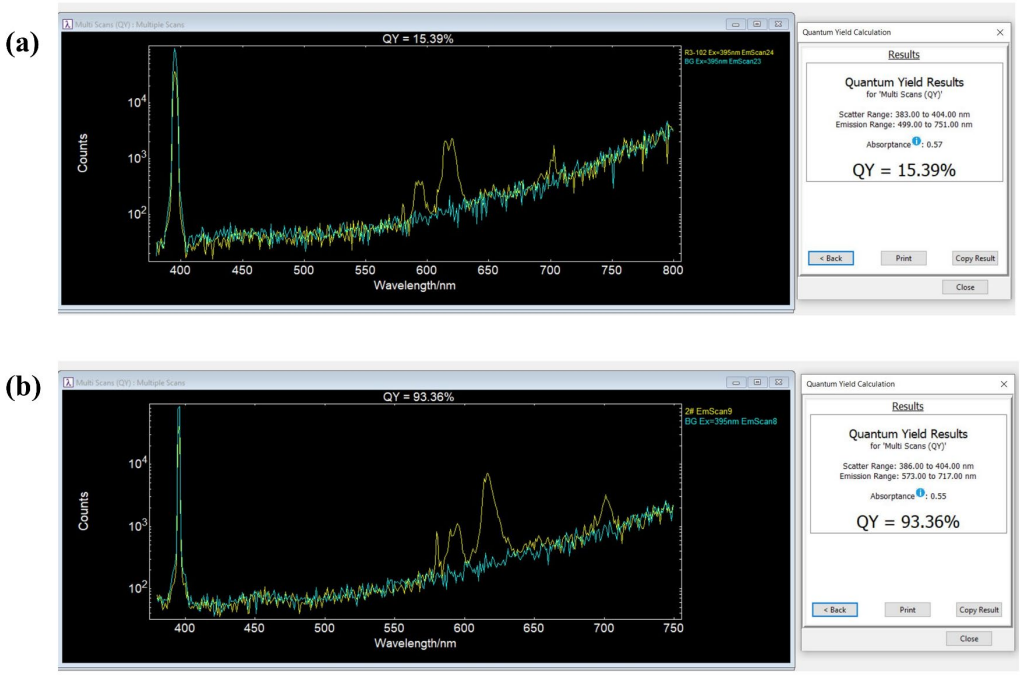

Figure S14. Original graph of quantum yield of **1-Eu** (a) and **2-Eu** (b).

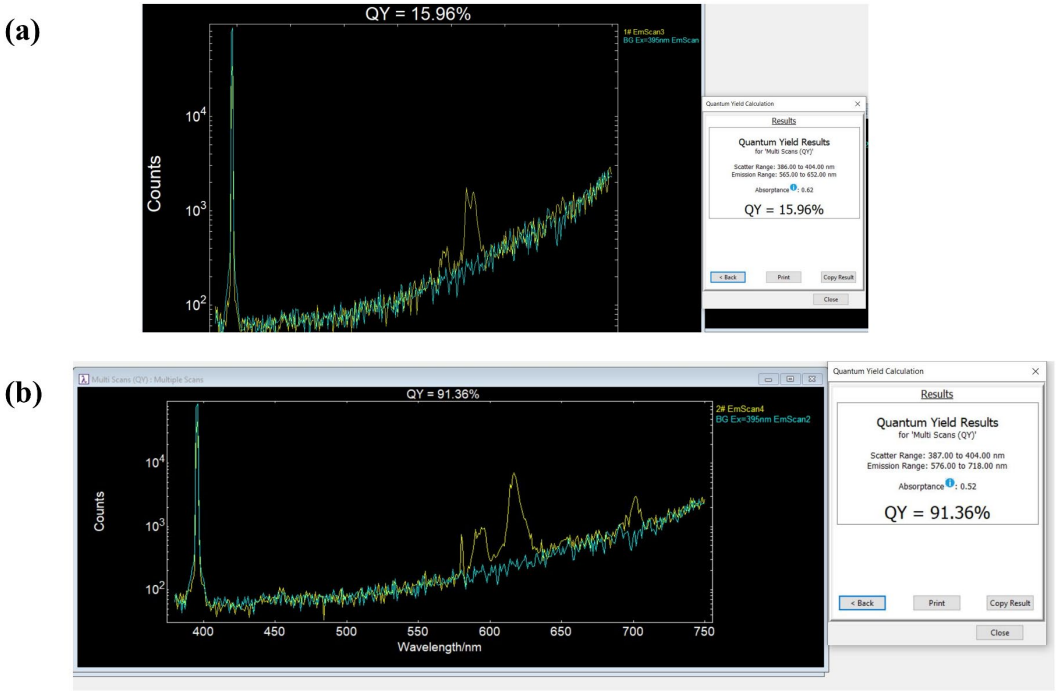

Figure S15. Original graph of quantum yield of **1-Eu** (a) and **2-Eu** (b) after 48 h exposure to 395 nm UV.

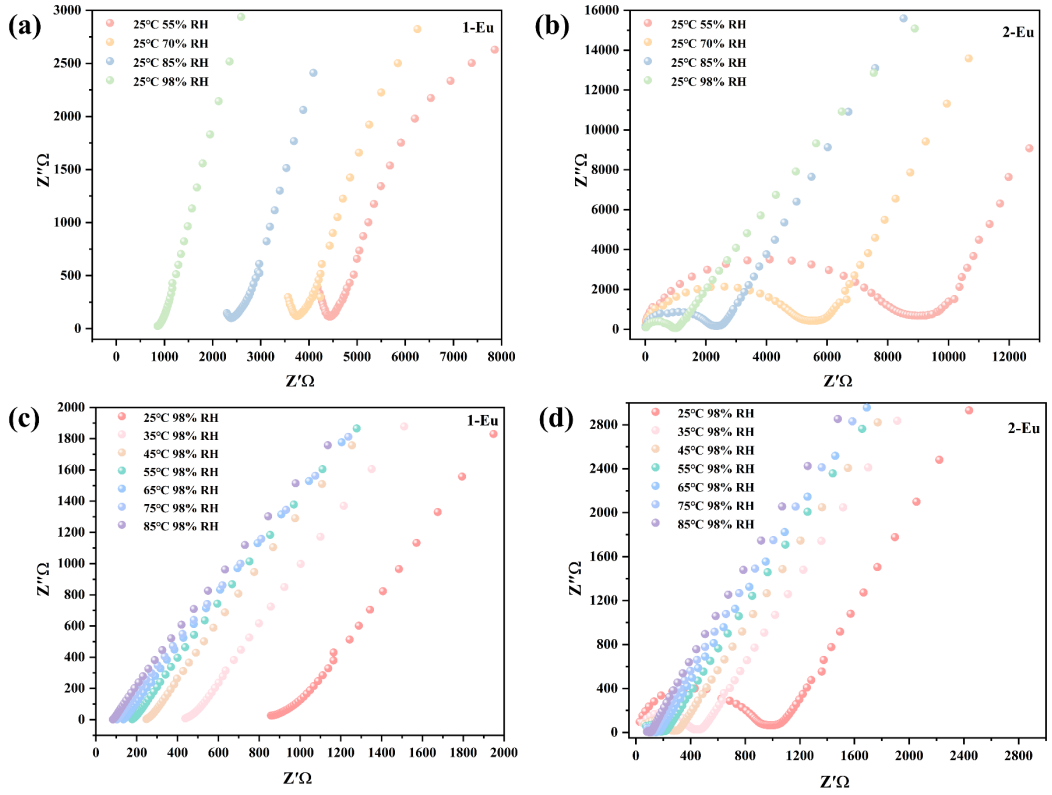

Figure S16. Nyquist plots at 55-98% RH and 298 K for **1-Eu** (a) and **2-Eu** (b). Nyquist plots at 25°C -85°C and 98% RH for **1-Eu** (c) and **2-Eu** (d).

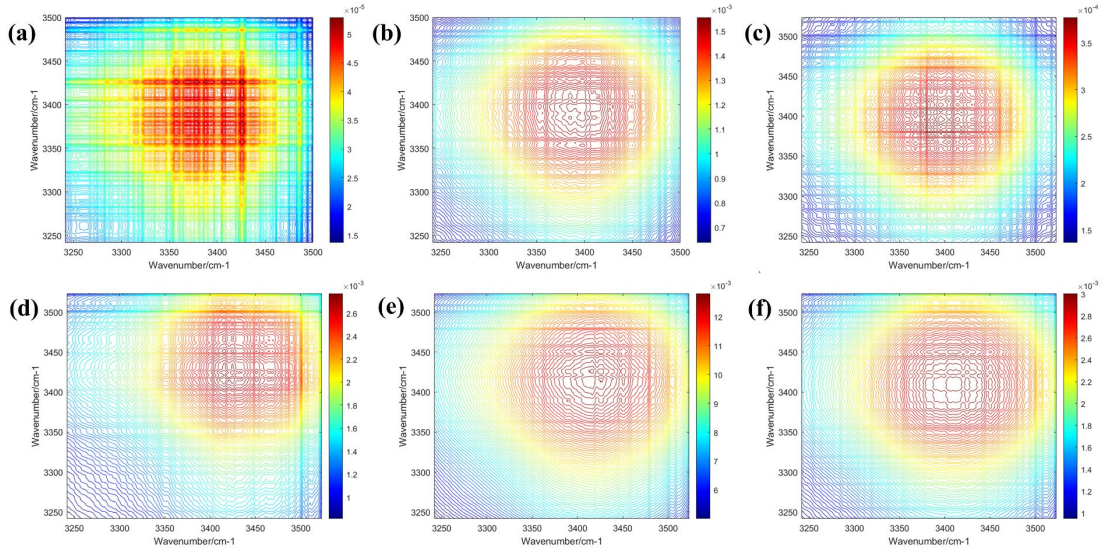

Figure S17. Synchronous two-dimensional correlation infrared spectra of **1-Eu** (a) and **2-Eu** (d) under 20-50 °C thermal perturbation. 2D COS-IR spectra of **1-Eu** (b) and **2-Eu** (e) under 50-90 °C thermal perturbation. 2D COS-IR spectra of **1-Eu** (c) and **2-Eu** (f) under 90-120 °C thermal perturbation.

In the two-dimensional infrared spectra under thermal perturbation, the intensities of the ν_{as}(O-H) response peaks for both compounds increase within the temperature

intervals of 20-50 °C and 50-90 °C, respectively. This indicates that from 20 °C to 90 °C, the hydrogen-bond vibrations are enhanced with rising temperature. In contrast, in the 90-120 °C range, the intensity of the v_{as}(O-H) response peaks decreases compared to that in the 50-90 °C interval. This reduction is attributed to the disruption of hydrogen bonds due to the loss of water molecules, leading to a corresponding decrease in the spectral.

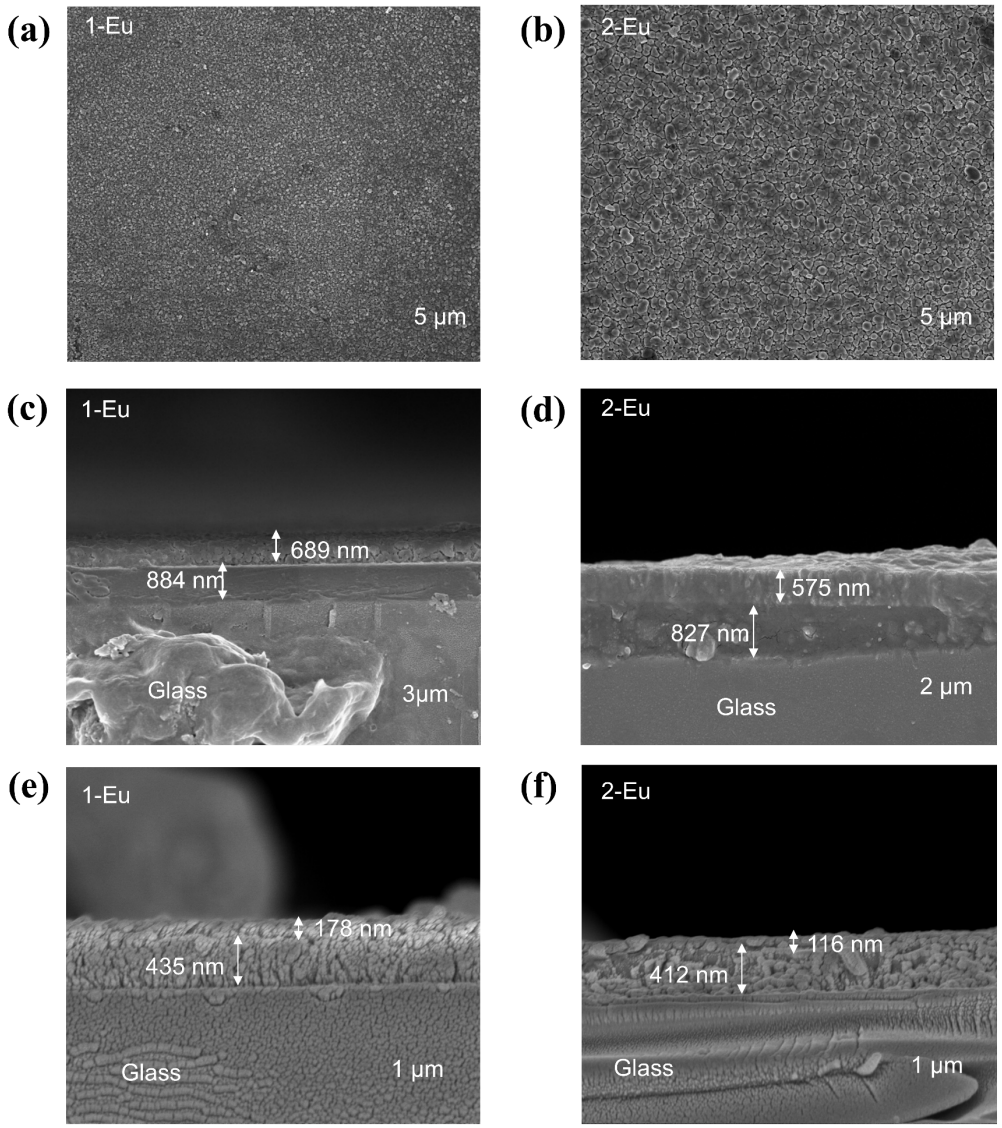

Figure S18. The surface SEM image of the (a) FTO/**1-Eu**/Ag; (b) FTO/**2-Eu**/Ag memory device. The cross-sectional SEM images of the (c) and (e) FTO/**1-Eu**/Ag; (d) and (f) FTO/**2-Eu**/Ag memory device.

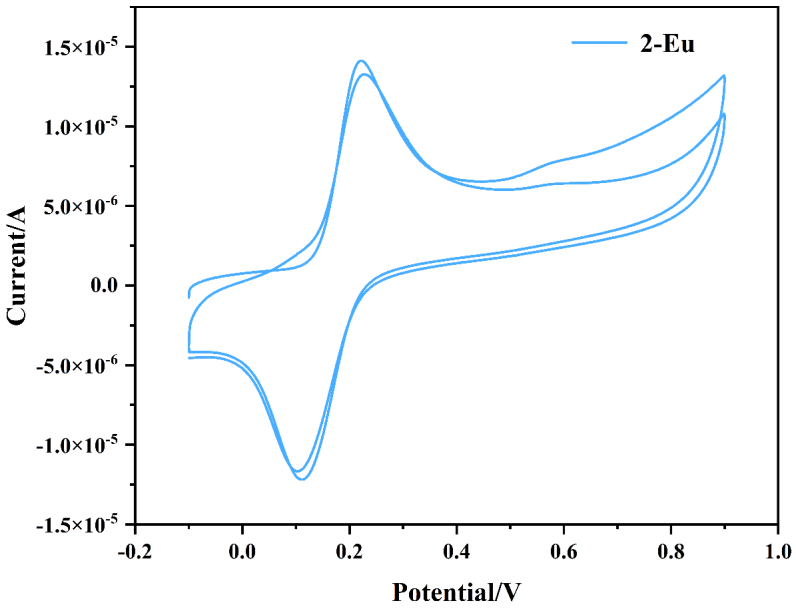

Figure S19. CV curves of **2-Eu**.

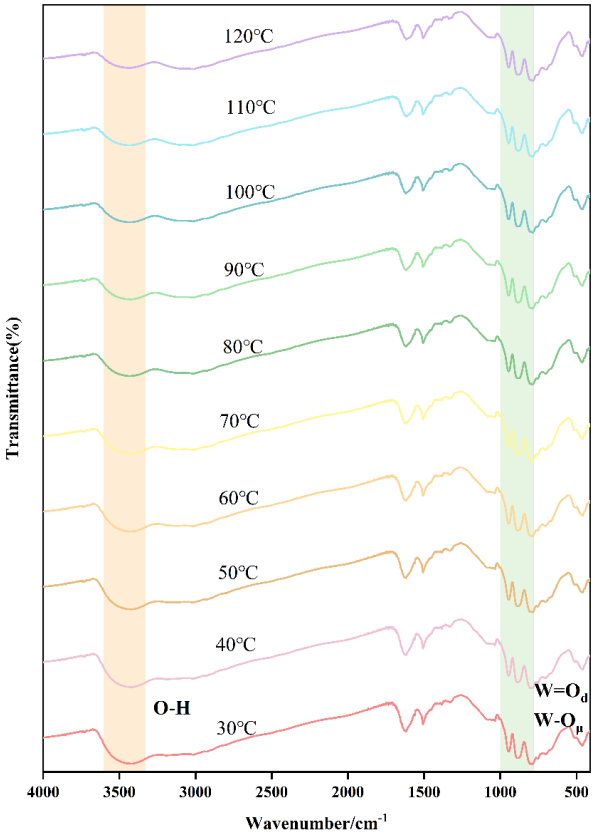

Figure S20. Temperature-dependent IR spectra of **2-Eu**.

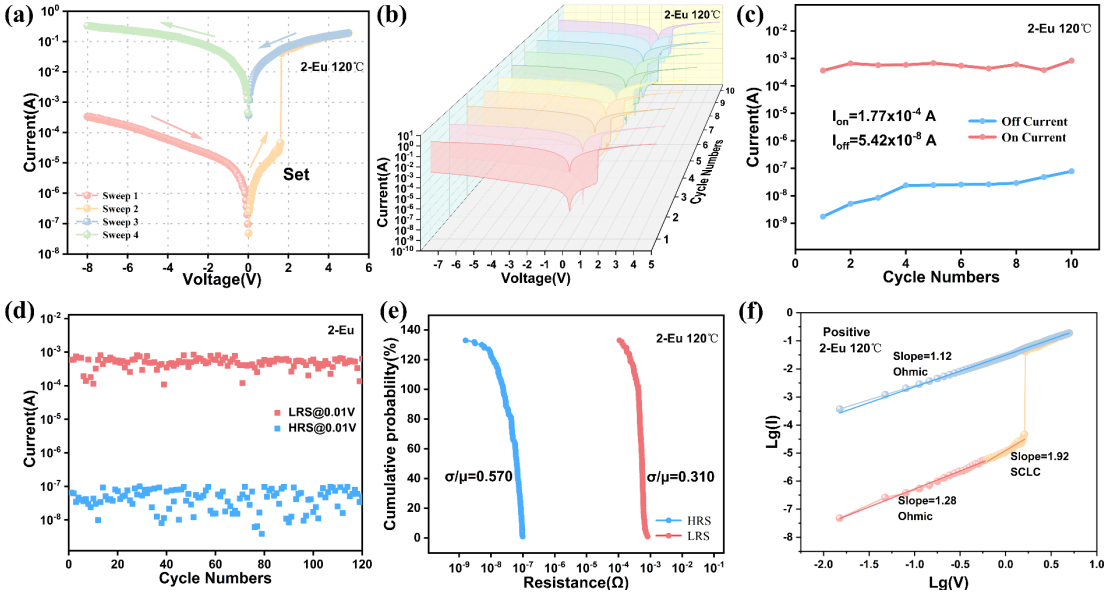

Figure S21. (a) *I-V* characteristics of FTO/**2-Eu**/Ag device at 120°C; (b) The *I-V* curves of 10 random samples of FTO/**2-Eu**/Ag device at 120°C; (c) Stabilities of 10 random samples FTO/**2-Eu**/Ag device at HRS and LRS states (read at 0.01V) at 120°C; (d) The endurance performance of device in HRS and LRS at 120°C; (e) The cumulative probability (CP) distributions of the HRS and LRS values for the device at 120°C; (f) Double logarithmic plot of the typical *I-V* characteristics in the positive voltage sweeping regions of FTO/2-**Eu**/Ag at 120°C.

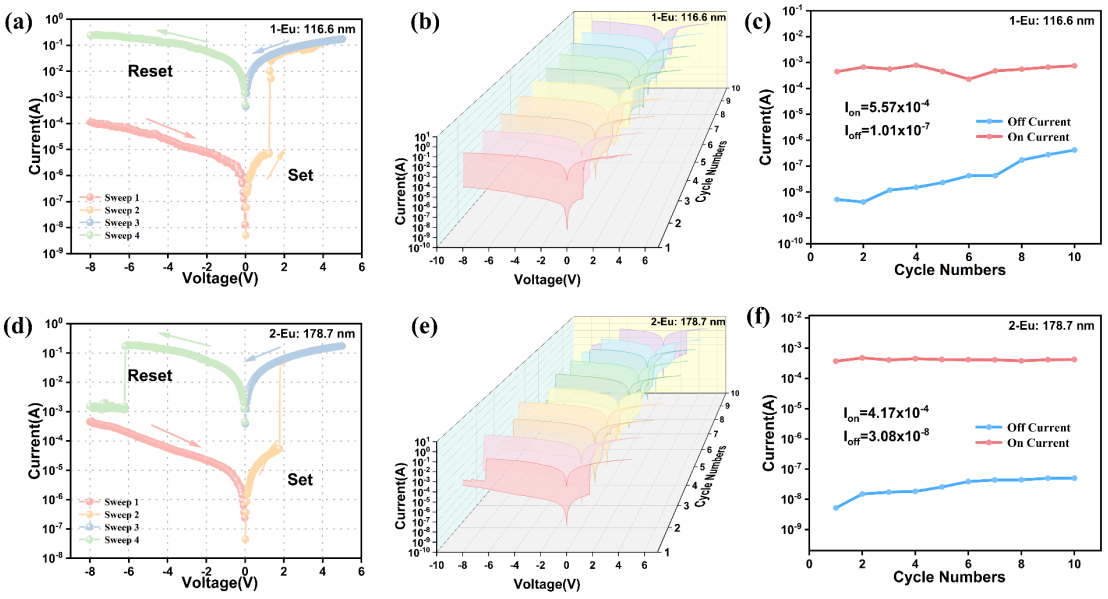

Figure S22. For FTO/**1-Eu**/Ag device (thickness: 116.6 nm): (a) *I-V* characteristic of a single device; (b) *I-V* curves of 10 random samples; (c) Stability of HRS and LRS states for 10 random samples (read at 0.01 V). For FTO/**2-Eu**/Ag device (thickness: 178.7 nm): (d) *I-V* characteristic of a single device; (b) *I-V* curves of 10 random samples; (c) Stability of HRS and LRS states for 10 random samples (read at 0.01 V).

To further evaluate the effect of thickness scaling on device performance and its relevance to miniaturization, thinner devices with active-layer thicknesses of approximately 100-200 nm were fabricated and tested. At the same measurement position, one *I-V* sweep was recorded every 2 min, and 10 consecutive I–V curves were collected for each device (Figure S20). Both devices preserved their original switching modes after thickness reduction: FTO/**1-Eu**/Ag showed WORM switching with an ON/OFF ratio of 5.51×10^3 and V_{SET} = 1.19 V, while FTO/**2-Eu**/Ag retained bipolar resistive switching with an ON/OFF ratio of 1.35×10^4, V_{SET} = 1.27 V, and V_{RESET} = -6.60 V. Compared with the thicker devices (500-700 nm), no significant degradation in the ON/OFF current switching ratio or switching voltage was observed, indicating that thickness reduction has a limited influence on device performance.

Section S5 Notes and references

1. S. Wang, T. Gong, Z. Wen, L. Chen and J. Zhao, First phosphite-bridging lanthanide–bismuth heterometallic selenotungstates and their ratio-metric-temperature luminescence sensing properties, *Journal of Materials Chemistry A*, 2025, **13**, 31530-31541.
2. S. Wang, T. Gong, L. Chen and J. Zhao, Pyrazine Dicarboxylic Acid and Phosphite-Bridging Lanthanide-Incorporated Tellurotungstates and Their Fluorescence Performances, *Inorganic Chemistry*, 2024, **63**, 20470-20481.
3. J. Wang, P. Ma, S. Li, Q. Xu, Y. Li, J. Niu and J. Wang, Polyoxotungstate Cluster Species Connected by Glutamic Acid and Europium, *Inorganic Chemistry*, 2019, **58**, 57-60.
4. S. Yang, T. Gong, Y. Dai, X. Xiao, J. Liu, L. Chen and J. Zhao, An Unusual Bismuth–Antimony–Europium Cluster-Imbedded Polyoxotungstate and Its Bidirectional Luminescence Detection, *Inorganic Chemistry*, 2023, **62**, 17861-17869.
5. Y.-F. Cao, W.-J. Xia, Y.-Q. Sun, X.-X. Li and S.-T. Zheng, Two polyoxotungstates containing lantern-shaped Eu20-oxo nanocages for information encryption and proton conduction, *Chinese Chemical Letters*, 2025, 111978.
6. W.-J. Mi, X.-R. Zhou, G.-Q. Ke, Y.-P. Chen and H.-H. Li, Photoluminescence Properties and Stable Bipolar Resistive Switching Behavior of Two Eu(III)-Doped Hexameric Selenotungstates, *Inorganic Chemistry*, 2025, **64**, 19647-19659.
7. Z. Li, Z.-H. Lv, H. Yu, Y.-Q. Sun, X.-X. Li and S.-T. Zheng, Giant Ln30-Cluster-Embedded Polyoxotungstate Nanoclusters with Exceptional Proton-Conducting and Luminescent Properties, *CCS Chemistry*, 2022, **4**, 2938-2945.
8. Q. Shang, K. Shen, D. Zhao, X. Wang, Y. Wei, H. Wang, G. Wang, D. Zhang and J. Niu, Rare-earth-induced peroxo-phosphotungstates: Enhanced proton conductivity in corresponding membranes, *Polyoxometalates*, 2025, **4**, 9140077.
9. P. M. Unnikrishnan, G. Premanand and S. K. Das, Polyoxometalate-driven assembly of inorganic–organic hybrid materials: Proton conductivity studies, *Journal of Chemical Sciences*, 2025, **137**, 13.
10. W. Lei, H. Li, M. Yang, J. Liu, W. Chen, P. Ma, J. Niu and J. Wang, Controllable Synthesis and Ultrahigh Proton Conduction of a Hydrogen-Bond Network, *Inorganic Chemistry*, 2024, **63**, 20492-

20500.

11. H.-P. Xiao, R.-T. Zhang, Z. Li, Y.-F. Xie, M. Wang, Y.-D. Ye, C. Sun, Y.-Q. Sun, X.-X. Li and S.-T. Zheng, Organoamine-Directed Assembly of 5p–4f Heterometallic Cluster Substituted Polyoxometalates: Luminescence and Proton Conduction Properties, *Inorganic Chemistry*, 2021, **60**, 13718-13726.
12. J.-H. Liu, L.-D. Lin, G.-Q. Wang, L.-Y. Li, Y.-Q. Sun, X.-X. Li and S.-T. Zheng, All-inorganic open frameworks based on gigantic four-shell Ln@W8@Ln8@(SiW12)6 clusters, *Chemical Communications*, 2020, **56**, 10305-10308.
13. B. Chen, Y.-R. Huang, K.-Y. Song, X.-L. Lin, H.-H. Li and Z.-R. Chen, Molecular Nonvolatile Memory Based on [α-GeW12O40]4–/Metalloviologen Hybrids Can Work at High Temperature Monitored by Chromism, *Chemistry of Materials*, 2021, **33**, 2178-2186.
14. Y.-R. Huang, X.-L. Lin, B. Chen, H.-D. Zheng, Z.-R. Chen, H.-H. Li and S.-T. Zheng, Thermal-Responsive Polyoxometalate–Metalloviologen Hybrid: Reversible Intermolecular Three-Component Reaction and Temperature-Regulated Resistive Switching Behaviors, *Angewandte Chemie International Edition*, 2021, **60**, 16911-16916.
15. H.-B. Chen, M.-Y. He, T. Li, C.-C. Deng, H.-P. Xiao, M.-Q. Qi, X.-J. Kong, H.-H. Li, X.-X. Li and S.-T. Zheng, Exploring the role of viologen and iodocuprate in the enhanced resistive switching performance of Anderson polyoxometalate-based three-component hybrids, *Journal of Materials Chemistry C*, 2024, **12**, 13555-13561.
16. Y.-F. Cao, Y.-J. Lin, X.-X. Li, Y.-Q. Sun and S.-T. Zheng, Two resistance-switchable hybrid polyoxotantalates based on {Co2Ta12} clusters, *CrystEngComm*, 2024, **26**, 3527-3534.
17. Y.-J. Wang, N. Shi, C. Sun, Y.-Q. Sun and S.-T. Zheng, Reversible Thermochromism and Stable Resistance Switching Behaviors Based on a Co(III)-Complex-Linked Polyoxoniobate, *Inorganic Chemistry*, 2023, **62**, 10675-10683.